Optimal Downlink Transmission for Cell-Free SWIPT Massive MIMO Systems with Active Eavesdropping

Mahmoud Alageli, Aissa Ikhlef, *Senior Member, IEEE*, Fahad Alsifiany, Mohammed A. M. Abdullah, *Member, IEEE*, Gaojie Chen, *Senior Member, IEEE* and Jonathon Chambers, *Fellow, IEEE*

***Abstract*—This paper considers secure simultaneous wireless information and power transfer (SWIPT) in cell-free massive multiple-input multiple-output (MIMO) systems. The system consists of a large number of randomly (Poisson-distributed) located access points (APs) serving multiple information users (IUs) and an information-untrusted dual-antenna active energy harvester (EH). The active EH uses one antenna to legitimately harvest energy and the other antenna to eavesdrop information. The APs are networked by a centralized infinite backhaul which allows the APs to synchronize and cooperate via a central processing unit (CPU). Closed-form expressions for the average harvested energy (AHE) and a tight lower bound on the ergodic secrecy rate (ESR) are derived. The obtained lower bound on the ESR takes into account the IUs' knowledge attained by downlink effective precoded-channel training. Since the transmit power constraint is per AP, the ESR is nonlinear in terms of the transmit power elements of the APs and that imposes new challenges in formulating a convex power control problem for the downlink transmission. To deal with these nonlinearities, a new method of balancing the transmit power among the APs via relaxed semidefinite programming (SDP) which is proven to be rank-one globally optimal is derived. A fair comparison between the proposed cell-free and the colocated massive MIMO systems shows that the cell-free MIMO outperforms the colocated MIMO over the interval in which the AHE constraint is low and vice versa. Also, the cell-free MIMO is found to be more immune to the increase in the active eavesdropping power than the colocated MIMO.**

***Index Terms*—Cell-free massive MIMO, SWIPT, active eavesdropping, secrecy, energy harvesting, artificial noise**

I. Introduction

In contrast to multi-cell massive multiple-input multiple-output (MIMO) systems in which the users in each cell (of a confined area) are served by an array of colocated antennas, cell-free massive MIMO is an architecture in which the users over a large area are served by a large number of distributed antennas (access points (APs)) [1]. Given the provision of backhaul phase-coherent cooperation between the APs [2]–[4], the distributed deployment of the APs offers many advantages such as: eliminating the correlation between the transmitting antennas, the ability to overcome deep shadow fading, and more importantly, large freedom in balancing the simultaneous transmissions of information, jamming and energy signals.

In massive MIMO systems, the asymptotic orthogonality between independent users' channels makes downlink transmission very robust against passive eavesdropping attacks [5]. Therefore, the active eavesdropping attack in massive MIMO systems (which introduces correlation between the estimated channels of both the attacker and the attacked user) is relevant. Active information-eavesdropping relies on attacking the uplink channel estimation phase by sending an identical training sequence as the legitimate information user (IU), such that the estimated IU's channel is correlated with the channel of the attacking eavesdropper (EV). Therefore, the active EV benefits from the downlink transmission which is beamformed based on the estimated IU's channel [5], [6].

The broadcast nature of the wireless channel imposes challenges in securing wireless communication systems, particularly, in the presence of adversarial EVs [7]. One example of such systems is simultaneous wireless information and power transfer (SWIPT) systems that comprise information-untrusted EHs. The secrecy issue in SWIPT massive MIMO systems, particularly under active attack, has previously lacked in-depth study in the literature. The main body of research concerning the secrecy problems in SWIPT systems has considered the colocated massive MIMO architecture [8]–[11]. Throughout the literature, much of the research regarding optimizing the performance of cell-free MIMO systems deals with the spectral efficiency [2, and the references therein], the energy efficiency [12]–[14], and the secrecy rate of wire-taped systems [15].

This paper investigates the design and the performance evaluation of SWIPT in cell-free massive MIMO, particularly, the secrecy of the information transmission under an active attack from a dual-antenna information-untrusted EH. From the service provider (cooperative APs) point of view, the dual-antenna active EH's request for service equivalently appears as a separate legitimate EH using a training power ϕP_E (where $0 < \phi < 1$ and P_E is the total available training power) via the energy harvesting antenna, and illegitimate active EV attacking

This work was supported by EPSRC grant number EP/R006377/1 ("M3NETs").

M. Alageli is with the Faculty of Engineering, Garaboulli, Elmergib University, Libya. (e-mail: alageli964@gmail.com).

F. Alsifiany is with the Intelligent Sensing and Communications Group, Newcastle University, NE1 7RU, UK. (e-mail: f.a.n.alsifiany2@ncl.ac.uk).

A. Ikhlef is with the Department of Engineering, Durham University, Durham, DH1 3LE, UK. (e-mail: aissa.ikhlef@durham.ac.uk).

M. A. M. Abdullah, G. Chen, and J. A. Chambers are with the School of Engineering, University of Leicester, Leicester, U.K., LE1 7RH (email: {m.abdullah, gaojie.chen and jonathon.chambers}@leicester.ac.uk). Mohammed A. M. Abdullah is also a staff member with the Computer and Information Engineering Department, Ninevah University, Mosul, 41002, Iraq (email: mohammed.abdulmuttaleb@uoninevah@edu.iq). J. A. Chambers is also with the College of Automation, Harbin Engineering University, China.

a certain IU with training power $(1-\phi)P_E$. However, the cooperative APs can rely on their large dimensionality to monitor the levels of training powers, therefore, they can blame the legitimate EH for the active attack. Instead of dropping the IU under attack from service, i.e., to stop sending information to the IU being attacked, the cooperative APs deal with the case by optimising the secrecy of the downlink transmission. Taking this action is useful and practical, particularly with the advantage of the large dimensionality of the APs.

Contributions: We are motivated by the lack of literature on the security of cell-free MIMO systems to provide a new globally optimal solution to the problem of joint power and data transfer in a cell-free massive MIMO system. The proposed system is established by a large number of randomly (Poisson-distributed) located APs which cooperate via a central processing unit (CPU). The communication links between the APs and the IUs are vulnerable to be wire-tapped by an information-untrusted dual-antenna active EH. Since the transmit power constraint is per AP, the secrecy rate is nonlinear in terms of the transmit power elements of the APs and that imposes new challenges in formulating a convex power control problem for the downlink transmission. The main contributions of our work are: 1) To jointly improve the ESR and the AHE (of the legitimate EH), we propose optimized downlink transmissions of three different signals: information, AN and energy signals beamformed towards the IUs, legitimate and illegitimate antennas of the EH, respectively; 2) We derive closed-form expressions for the AHE and a tight lower bound on the ESR. The derived expressions are deterministic at the CPU and take into account the IUs' knowledge attained by downlink effective precoded-channel training; 3) Knowing that the ESR is nonlinear in terms of the transmit power elements of the APs, a new globally optimal iterative method for cooperatively balancing the transmit powers at the APs via relaxed semidefinite programming (SDP) is derived; 4) We provide a proof for the rank-one global optimality of our SDP solution (Theorem 3) and the convergence of our iterative SDP problem (Subsection IV-C2); 5) Finally, a fair performance comparison between the proposed cell-free and colocated massive MIMO systems is performed. The comparison shows informative results of the secrecy performance with respect to the active eavesdropping training power and the range of the AHE constraint values.

Related Work: To the best of the authors' knowledge, the secrecy performance in cell-free massive MIMO systems has only been studied in [15] where the focus was on maximizing the secrecy rate of a given IU when being attacked by an active EV under constraints on the individual rates of all IUs. We can compare the work in this paper to the work in [15] from two perspectives: 1) From system and signal design perspectives, our work considers the worst-case SWIPT problem by optimizing three different downlink signals: information, AN and energy signals beamformed towards the IUs, legitimate and illegitimate antennas of the dual-antenna EH, respectively; while the work in [15] considers the secrecy problem of a certain IU by optimizing the downlink information signals (no jamming or power transfer are considered); 2) From a problem-solving perspective, the employed lower bound on the secrecy rate in [15] imposes constraints on the domain of the linear programming (LP) optimization variables (the allocated power of the downlink information vectors) [15, (23)], i.e., the values of allocated power vectors are feasible on a sub-region of $\mathcal{R}_+^N$, where N is the total number of APs. Since the update in the proposed iterative algorithm does not include the power vector of the considered IU, the obtained solution is locally optimal, or at least, the globally optimal solution is not guaranteed. In contrast, in our work, both the objective function and constraints of the SDP formulation are differentiable and there are no constraints on the domain of the optimization variables which implies the satisfaction of Slater's condition. Therefore, by proving the optimal rank requirements (please see Theorem 3 and its proof) and the convergence of the employed iterative problem (please see Subsection IV-C2), we claim the global optimality of our solution. In our early work in [11], an active dual-antenna information-untrusted EH (equivalent to the proposed EH in this paper) has been considered for a colocated SWIPT massive MIMO system. However, considering such a secrecy problem for cell-free massive MIMO will result in a non-linear objective function in terms of the allocated power elements at the APs. Inevitably, this problem can not be solved by the LP method used for a colocated massive MIMO in [11], and this leads to a completely different SDP optimization challenge.

Notation: Vectors and matrices are denoted by boldface lower case and boldface upper case letters, respectively. $\boldsymbol{I}_N$ denotes the $N \times N$ identity matrix. $\text{diag}(\boldsymbol{s})$ is a matrix whose diagonal entries are the entries of vector $\boldsymbol{s}$ and zeros elsewhere. $\text{diag}(\boldsymbol{S})$ is a column vector whose entries are the diagonal entries of matrix $\boldsymbol{S}$. $\boldsymbol{S} \succeq 0$ indicates that $\boldsymbol{S}$ is a positive semidefinite matrix. The operators $(\cdot)^T$, $(\cdot)^H$, $\text{tr}(\cdot)$, $\log_2(\cdot)$ and $|\cdot|$ denote the transpose, conjugate transpose, trace of a matrix, logarithm to base 2 and the absolute value of scalars, respectively. $\mathcal{R}$, $\mathcal{R}_+^n$, $\mathcal{S}_+^n$ and $\mathcal{C}^{m\times n}$ denote the sets of real numbers, nonnegative real numbers, symmetric positive semidefinite $n \times n$ real matrices and complex $m \times n$ matrices, respectively. $\boldsymbol{x} \sim \mathcal{CN}(\boldsymbol{0}, \boldsymbol{\Sigma})$ denotes a circularly symmetric complex Gaussian random vector $\boldsymbol{x} \in \mathcal{C}^{N\times 1}$ with zero mean and covariance matrix $\boldsymbol{\Sigma}$. $\text{cov}(x, y)$ and $\text{var}(x)$ denote the covariance between the random variables x and y, and the variance of x, respectively. $\{\boldsymbol{a}_n\}$ denotes a set of all vectors indexed by n. $\{a_{m,n}\}_m$ denotes a set of all scalars indexed by m. $[\boldsymbol{a}]_n$ and $[\boldsymbol{A}]_{n,m}$ indicate the nth entry of $\boldsymbol{a}$ and the nth entry of the mth column of $\boldsymbol{A}$, respectively. $f(N) \overset{N\to\infty}{\to} a$ is equivalent to $\lim_{N\to\infty} f(N) = a$. $[x]^+ = \max(x, 0)$. $\boldsymbol{B} = \text{null}(\boldsymbol{A})$ means $\boldsymbol{AB} = \boldsymbol{0}$ and $\boldsymbol{BB}^H = \boldsymbol{I}$.

II. System Model

As illustrated in Fig. 1, we consider the downlink of a cell-free massive MIMO system consisting of a large number of APs which are randomly located on a two dimensional Euclidean area A_a based on an homogeneous Poisson point process (PPP) Φ_a with an intensity λ_a; M single antenna IUs interested in information decoding, $\{\text{IU}_i\}$, $i = 1, 2, ..., M$; and an active information-untrusted EH, equipped with two antennas, where one antenna is used to legitimately harvest

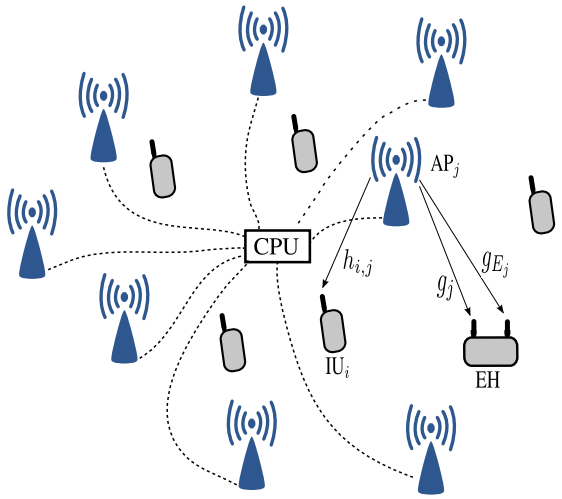

Fig. 1. An illustration of the proposed SWIPT cell-free massive MIMO system, only a small number of APs is illustrated for clarity.

energy, while the other antenna is used to illegitimately and actively eavesdrop and decode an information signal intended for a certain IU, IU$_k$, $k \in \{1, 2, ..., M\}$. Unless otherwise stated, the IUs and the EH are randomly located on a two dimensional Euclidean area $\mathrm{A}_u < \mathrm{A}_a$[1]. The origins of both A_u and A_a coincide. The APs are networked by a centralized infinite backhaul that allows them to synchronize and cooperate via a CPU.

Let $\{\mathrm{AP}_1, \ \ldots, \mathrm{AP}_N\}$ be the set of the adopted realization of APs. $\boldsymbol{h}_i = [h_{i,1}, \ \ldots, h_{i,N}]^T = \boldsymbol{\Gamma}_i^{\frac{1}{2}} \bar{\boldsymbol{h}}_i$ denotes the uplink channel vector between IU$_i$ and the set of APs, where $\bar{\boldsymbol{h}}_i \sim \mathcal{CN}(\boldsymbol{0}, \boldsymbol{I}_N)$ is the small-scale fading vector and $\boldsymbol{\Gamma}_i = \mathrm{diag}([\gamma_{i,1}, \ \ldots, \gamma_{i,N}])$, $\gamma_{i,j}$ is the large-scale fading coefficient of the channel between IU$_i$ and AP$_j$. $\boldsymbol{g} = [g_1, \ \ldots, g_N]^T = \boldsymbol{\Gamma}^{\frac{1}{2}} \bar{\boldsymbol{g}}$ and $\boldsymbol{g}_E = [g_{E_1}, \ \ldots, g_{E_N}]^T = \boldsymbol{\Gamma}^{\frac{1}{2}} \bar{\boldsymbol{g}}_E$ denote the uplink channel vectors between the legitimate and the illegitimate (eavesdropping) antennas of the EH and the set of APs, respectively, where $\bar{\boldsymbol{g}} = [\bar{g}_1, \ \ldots, \bar{g}_N]^T$, $\bar{\boldsymbol{g}}_E = [\bar{g}_{E_1}, \ \ldots, \bar{g}_{E_N}]^T \sim \mathcal{CN}(\boldsymbol{0}, \boldsymbol{I}_N)$ are independent, uncorrelated small-scale fading vectors. $\boldsymbol{\Gamma} = \mathrm{diag}([\gamma_1, \ \ldots, \gamma_N])$ where γ_j is the large-scale fading coefficient of the channel between the EH and AP$_j$. The large-scale fading coefficients $\{\gamma_{i,j}, \ \gamma_j\}$ change very slowly compared to the small-scale fading coefficients, therefore, we assume that $\{\gamma_{i,j}, \ \gamma_j\}$ are perfectly known at the APs [16].

A. Uplink Channel Estimation

The user small-fading channels manifest block fading, i.e., they remain constant over one time block, but change independently from one block to another. Each time block is divided into three time slots of lengths: τ transmission samples for uplink training, τ_d transmission samples for downlink training and τ_s samples for downlink data transmission. Without loss of generality, we assume a unit time slot for the downlink data transmission $\tau_s T_s = 1s$, where T_s is the duration of the transmitted data symbol [8], [17]. During the uplink training phase, a training sequence is sent from each IU with an average power P_I. Pessimistically, we assume that the EH has the potential to acquire the training sequence of a certain IU (made possible by overhearing the leaking electromagnetic signalling between the APs and the IUs [18]). Therefore, the EH sends a copy of the training sequence of the attacked IU, IU$_k$, $k \in \{1, 2, \ \ldots, M\}$, via its eavesdropping antenna using part of its total average power ϕP_E, $0 < \phi < 1$, such that the cooperative APs estimate the uplink composite channel coefficients of both IU$_k$ and the eavesdropping antenna of the EH. Consequently, the estimated channel of IU$_k$ will be corrupted and correlated with the illegitimate channel of the EH [5], [19]. The remaining training power $(1-\phi)P_E$ is used for transmitting the legitimate uplink training sequence via the energy harvesting antenna. The uplink training sequences of the IUs and legitimate EH are assumed to be orthogonal. The signal at the APs received across τ training transmissions is

$$\boldsymbol{Y} = \sum_{i=1}^{M} \sqrt{P_I}\, \boldsymbol{h}_i\, \boldsymbol{\psi}_i^T + \sqrt{\phi P_E}\boldsymbol{g}_E \boldsymbol{\psi}_k^T + \sqrt{(1-\phi)P_E}\boldsymbol{g}\boldsymbol{\psi}_E^T + \boldsymbol{N}, \tag{1}$$

where $\boldsymbol{N} \in \mathcal{C}^{N\times\tau}$ is the additive noise matrix with entries following the distribution $\mathcal{CN}(0, \sigma_n^2)$. k is the index of the attacked IU, IU$_k$. $\boldsymbol{\psi}_i, \ \boldsymbol{\psi}_k, \ \boldsymbol{\psi}_E \in \mathcal{C}^{\tau\times 1}$ are the uplink training sequences of IU$_i$, the IU under attack, IU$_k$, and the legitimate antenna of the EH, respectively. $\boldsymbol{\psi}_i^H \boldsymbol{\psi}_{j\neq i}, \ \boldsymbol{\psi}_i^H \boldsymbol{\psi}_E = 0$; and $\boldsymbol{\psi}_i^H \boldsymbol{\psi}_i, \ \boldsymbol{\psi}_E^H \boldsymbol{\psi}_E = \tau$. We assume centralized channel estimation via the CPU. Given that IU$_k$ is the attacked IU, the minimum mean square error (MMSE) estimate of $\boldsymbol{h}_i$, $\hat{\boldsymbol{h}}_i = [\hat{h}_{i,1}, \ \ldots, \hat{h}_{i,N}]^T$, and of $\boldsymbol{g}$, $\hat{\boldsymbol{g}} = [\hat{g}_1, \ \ldots, \hat{g}_N]^T$, are given as

$$\hat{\boldsymbol{h}}_i = \boldsymbol{C}_i \boldsymbol{y}_i, \ \boldsymbol{C}_i = \sqrt{P_I}\boldsymbol{\Gamma}_i \left(\tau P_I \boldsymbol{\Gamma}_i + \delta_{ik}\, \tau\phi P_E \boldsymbol{\Gamma} + \sigma_n^2 \boldsymbol{I}_N\right)^{-1}, \tag{2a}$$

$$\boldsymbol{y}_i = \boldsymbol{Y}\boldsymbol{\psi}_i^* = \tau\sqrt{P_I}\boldsymbol{h}_i + \delta_{ik}\, \tau\sqrt{\phi P_E}\, \boldsymbol{g}_E + \boldsymbol{N}\boldsymbol{\psi}_i^*, \tag{2b}$$

$$\hat{\boldsymbol{g}} = \boldsymbol{C}\boldsymbol{y}, \quad \boldsymbol{C} = \sqrt{(1-\phi)P_E}\boldsymbol{\Gamma} \ \left(\tau(1-\phi)P_E \boldsymbol{\Gamma} + \sigma_n^2 \boldsymbol{I}_N\right)^{-1}, \tag{2c}$$

$$\boldsymbol{y} = \boldsymbol{Y}\boldsymbol{\psi}_E^* = \tau\sqrt{(1-\phi)P_E}\, \boldsymbol{g} + \boldsymbol{N}\boldsymbol{\psi}_E^*, \tag{2d}$$

where $\delta_{ik} = 1$ if $i = k$ (i.e., IU$_i$ is the attacked IU) and $\delta_{ik} = 0$ if $i \neq k$. The covariance matrices $\mathbb{E}[\hat{\boldsymbol{h}}_i \hat{\boldsymbol{h}}_i^H]$ and $\mathbb{E}[\hat{\boldsymbol{g}}\hat{\boldsymbol{g}}^H]$ are equal to $\boldsymbol{R}_i = \tau\sqrt{P_I}\boldsymbol{\Gamma}_i\boldsymbol{C}_i$ and $\boldsymbol{R} = \tau\sqrt{(1-\phi)P_E}\boldsymbol{\Gamma}\boldsymbol{C}$, respectively. To emphasize whether IU$_i$ is being attacked or not, we use $\boldsymbol{R}_i$ to describe the covariance matrix of IU$_i$ if not being attacked and $\bar{\boldsymbol{R}}_i$ to describe the covariance matrix of IU$_i$ if being attacked. Both $\boldsymbol{R}_i$ and $\bar{\boldsymbol{R}}_i$ are calculated by the same aforementioned formula, but with $k \neq i$ for $\boldsymbol{R}_i$ and with $k = i$ for $\bar{\boldsymbol{R}}_i$. The results in (2a) and (2c) follow from standard channel estimation theory [20], [21]. Active eavesdropping attack detection and the identification of the attacked IU, IU$_k$, are possible and have been studied in [22]–[24]. Alternatively, the cooperative APs can exploit their large

[1]Since each user (IU or EH) is dominantly served by a subset of the APs, the assumption $\mathrm{A}_u < \mathrm{A}_a$ introduces an overlap between the dominant AP groups serving different users. From the secure SWIPT design point of view, this case is more severe than the case when the users are widely apart, i.e., $\mathrm{A}_u = \mathrm{A}_a$.

dimensionality to detect the active eavesdropping attack by monitoring the values of training powers which have been proven to be accurate as $N \to \infty$. The CPU can calculate the eavesdropping (illegitimate) and the legitimate training powers of the EH, ϕP_E and $(1-\phi)P_E$, respectively, by using the following lemma.[2]

Lemma 1: For a large density of APs as $\lambda_a \to \infty$, which leads to a large number of APs as $N \to \infty$, any illegitimate active training power can be identified and calculated as

$$\frac{\boldsymbol{y}_i^H \boldsymbol{y}_i - \tau^2 P_I \text{tr}\left(\boldsymbol{\Gamma}_i\right) - N\tau\sigma_n^2}{\tau^2 \text{tr}\left(\boldsymbol{\Gamma}\right)} \overset{N\to\infty}{\to} \delta_{ik}\ \phi P_E, \tag{3}$$

where IU_i is under attack if $\delta_{ik} = 1$, i.e., $k = i$, and IU_i is not being attacked if $\delta_{ik} = 0$, i.e., $k \neq i$. All the scalars, vector and matrices in the left-hand side of (3) are deterministic at the CPU.

Proof: See Appendix A. ∎

As will be seen in the next subsection, the downlink signal design at the cooperative APs does not require knowledge of which antenna is used for energy harvesting and which one is used for eavesdropping. The cooperative APs need to know the estimated channel of the IU under attack which can be identified by using Lemma 1, and the estimated channel of the legitimate energy harvesting antenna of the EH whose identification is possible since it uses a training sequence orthogonal to the training sequences of the other users.

B. Downlink Transmission

The APs cooperate via the CPU to control the power allocation of the downlink data, AN, and energy signal transmissions. From the service provider (cooperative APs) point of view, the EH's request for service equivalently appears to the cooperative APs as a separate legitimate EH which uses a training power ϕP_E and illegitimate active eavesdropper attacking a certain IU, IU_k, with a training power $(1-\phi)P_E$. However, the CPU relies on the large dimensionality of the APs to monitor the levels of training powers, and based on Lemma 1, it can blame the legitimate EH for the active attack. Upon the detection of the active attack, the CPU has no option but to deal with this attack, and only two possible actions might be taken:

- Dropping the IU under attack from service, i.e., to stop sending information to the IU being attacked. With an exception for IUs receiving information with a high degree of importance, such an action seems impractical. Therefore, there is no secrecy design for the downlink transmission.
- Dealing with the case by optimizing the secrecy of downlink transmission (by employing controlled transmissions of information, jamming and energy signals). Taking this action is useful and practical, particularly with the advantage of the large number of randomly located APs. Compared to the case of collocated APs (conventional MIMO), the average path-loss from an AP to the active EH and the attacked IU varies from one AP to another. This property of randomly distributed APs would increase the efficiency of power control in tackling the active eavesdropping.

Given that the IU_k is the attacked IU, the APs employ the matched filter (MF) precoder to transmit the downlink signal vector

$$\boldsymbol{x}_k = \sum_{i=1}^{M} \boldsymbol{w}_i q_i + \bar{\boldsymbol{w}}_k z + \boldsymbol{w}, \tag{4}$$

where the jth entry of $\boldsymbol{x}_k$, $[\boldsymbol{x}_k]_j$, is the signal transmitted by AP_j, $\boldsymbol{w}_i q_i$ is the information signal vector directed towards IU_i, $\bar{\boldsymbol{w}}_k z$ is the AN signal vector directed towards the eavesdropping antenna of the EH, and $\boldsymbol{w}$ is the energy signal vector directed towards the legitimate antenna of the EH. $\{q_i\}$ and z are the information signal symbols intended for $\{\text{IU}_i\}$ and the AN symbol, respectively, and they are mutually independent and follow the distribution $\mathcal{CN}(0,1)$. The MF beamforming vectors in (4) are defined as[3]

$$\boldsymbol{w}_i = \text{diag}\left(\boldsymbol{p}_i\right)\hat{\boldsymbol{h}}_i^*,\ \boldsymbol{p}_i = \left[\sqrt{p_{i,1}},\ \ldots,\ \sqrt{p_{i,N}}\right]^T, \tag{5a}$$

$$\bar{\boldsymbol{w}}_k = \text{diag}\left(\bar{\boldsymbol{p}}\right)\hat{\boldsymbol{h}}_k^*,\ \bar{\boldsymbol{p}} = \left[\sqrt{\bar{p}_1},\ \ldots,\ \sqrt{\bar{p}_N}\right]^T, \tag{5b}$$

$$\boldsymbol{w} = \text{diag}\left(\boldsymbol{p}\right)\hat{\boldsymbol{g}}^*,\ \boldsymbol{p} = \left[\sqrt{p_1},\ \ldots,\ \sqrt{p_N}\right]^T. \tag{5c}$$

For example, $|\left[\boldsymbol{w}_i\right]_j|^2 = p_{i,j}|\hat{h}_{i,j}|^2$, $|\left[\bar{\boldsymbol{w}}_k\right]_j|^2 = \bar{p}_j|\hat{h}_{k,j}|^2$ and $|\left[\boldsymbol{w}\right]_j|^2 = p_j|\hat{g}_j|^2$ are the allocated powers at AP_j for IU_i's data, AN and energy signals, respectively. Power allocation is controlled via the factors $\{p_{i,j}\}$, $\{\bar{p}_j\}$ and $\{p_j\}$. Referring to (2a) and (5b), it can be noticed that the received AN signal power at the eavesdropping antenna of the EH, $|\boldsymbol{g}_E^T\bar{\boldsymbol{w}}_k|^2$, is directly proportional to the eavesdropping training power, ϕP_E, i.e., the larger the eavesdropping training power, the larger the jamming received power by the EH. Therefore, although the AN is aligned to the IU_k's estimated channel coefficients, the cooperative APs can improve the information secrecy by exploiting the nature of the cell-free system – in which IU_k and the EH experience different path-losses to a single AP – by optimizing the per AP per user power control.

Given that IU_k is the attacked IU. The received signals at IU_i, $y_{k,i}$; the legitimate antenna of the EH, y_k; and at the eavesdropping antenna of the EH, y_{E_k}, are

$$y_{k,i} = \boldsymbol{h}_i^T\boldsymbol{x}_k + n_i,\ y_k = \boldsymbol{g}^T\boldsymbol{x}_k + \hat{n},\ y_{E_k} = \boldsymbol{g}_E^T\boldsymbol{x}_k + \bar{n}, \tag{6}$$

where n_i, $\hat{n}$ and $\bar{n}$ are zero mean σ_n^2 variance complex Gaussian noises at IU_i, the legitimate and eavesdropping antennas of the EH, respectively.

Remark 1: Although the AN signal might be designed for both actions of interfering eavesdropping antenna and providing wireless energy at the energy harvesting antenna [17], the cooperative APs transmit two different beamformed signals since the EH's request for service equivalently appears

[2]Since the cooperative APs are able to monitor the changes in the training powers of the IUs and the EH using Lemma 1, we assume that the cooperative APs blame the information-untrusted EH for the active eavesdropping attack.

[3]Please note, due to active attack, the $\hat{\boldsymbol{h}}_k$ used to design $\bar{\boldsymbol{w}}_k$ in (5b) is the estimate of the composite channel of both $\boldsymbol{h}_k$ and $\boldsymbol{g}_E$. By optimizing the per AP AN power factors $\{\bar{p}_1,\ \ldots,\ \bar{p}_N\}$, the AN power can be maximized at the EH and minimized at the IU_k.

to the cooperative APs as a separate legitimate EH and illegitimate active eavesdropper attacking a certain IU. We assign different names for the two signals since they are beamformed with different beamforming vectors: 1) $\bar{\boldsymbol{w}}_k$ (aligned to the composite estimated channel vector of the illegitimate antenna of the EH and the IU$_k$, $\hat{\boldsymbol{h}}_k$) for the AN signal (jamming signal) when the EH attacks IU$_k$; 2) $\boldsymbol{w}$ (aligned to the estimated channel vector of the legitimate antenna $\hat{\boldsymbol{g}}$) for the energy signal.

C. Downlink Effective Precoded-Channel Estimation

With a large number of APs, the channel estimation at all IUs requires training sequences of a length $\geq N$ which is practically infeasible. Alternatively, we propose the estimation of the effective precoded-channels, $\{a_{i,i} = \boldsymbol{h}_i^T \boldsymbol{w}_i\}$ at the IUs[4]. The downlink estimation of the effective precoded-channels at the IUs requires M orthogonal training sequences that can be of a finite length, $\geq M$. Therefore, such a downlink estimation is practically possible. Notice that IU$_i$ needs to estimate its effective precoded-channel $a_{i,i}$ which includes the values of power control factors $\{p_{i,j}\}$, $\{\bar{p}_j\}$ and $\{p_j\}$. Therefore the values of $\{p_{i,j}\}$, $\{\bar{p}_j\}$ and $\{p_j\}$ to be used for downlink data transmission are employed for downlink training. The cooperative APs transmit the downlink training signal matrix $\boldsymbol{X}_d = \sum_{i=1}^{M} \boldsymbol{w}_i \ \boldsymbol{\psi}_{d_i}^T$, where $\{\boldsymbol{\psi}_{d_i}\}$ ($\boldsymbol{\psi}_{d_i}^H \boldsymbol{\psi}_{d_i} = \tau_d$ and $\boldsymbol{\psi}_{d_i}^H \boldsymbol{\psi}_{d_{j\neq i}} = 0$) are the downlink training sequences of the IUs[5]. The received training signal vector at IU$_i$, $\boldsymbol{y}_{I_i} \in \mathcal{C}^{1\times\tau_d}$ is

$$\boldsymbol{y}_{I_i} = \boldsymbol{h}_i^T \boldsymbol{X}_d + \boldsymbol{n}_i = \sum_{j=1}^{M} a_{i,j} \boldsymbol{\psi}_{d_j}^T + \boldsymbol{n}_i, \tag{7}$$

where $a_{i,j} = \boldsymbol{h}_i^T \boldsymbol{w}_j$ and $\boldsymbol{n}_i \sim \mathcal{CN}(0, \sigma_n^2 \boldsymbol{I}_{\tau_d})$ is the noise vector at IU$_i$. First, let us examine the MMSE estimate of $a_{i,i}$ at IU$_i$ which can be calculated as [20], [21]

$$\frac{\boldsymbol{p}_i^T \boldsymbol{\Gamma}_i \boldsymbol{R}_i \boldsymbol{p}_i}{\boldsymbol{p}_i^T \boldsymbol{\Gamma}_i \boldsymbol{R}_i \boldsymbol{p}_i + \tau_d \sigma_n^2} \ y_{I_i}, \tag{8}$$

where $y_{I_i} = \boldsymbol{y}_{I_i} \boldsymbol{\psi}_{d_i}^* = \tau_d a_{i,i} + \boldsymbol{n}_i \boldsymbol{\psi}_{d_i}^*$. However, since the allocated power control factors in $\boldsymbol{p}_i$ are not available at IU$_i$, the calculation of (8) is not possible, and instead, we assume that IU$_i$ performs a simple least square error (LSE) estimate of $a_{i,i}$, $\hat{a}_{i,i}$ which is given as

$$\hat{a}_{i,i} = \frac{y_{I_i}}{\tau_d} = a_{i,i} + \tilde{a}_{i,i}, \tag{9}$$

where $\tilde{a}_{i,i} = \frac{\boldsymbol{n}_i \boldsymbol{\psi}_{d_i}^*}{\tau_d}$ is the estimation error which is statistically independent from the effective precoded channel $a_{i,i}$.

[4]The EH has the potential to estimate the precoded channel for the attacked IU, $b_k = \boldsymbol{g}_E^T \boldsymbol{w}_k$, however, as will be seen in Subsection III-B, the worst case in which the EH can perfectly estimate b_k is assumed.

[5]The same training sequences could be used in the uplink and downlink.

III. Secrecy Analysis

A. Lower Bound on the IU Rate

The received signal at IU$_i$, $y_{k,i}$, given in (6) can be recast as follows

$$\begin{aligned} y_{k,i} &= a_{i,i} q_i + Z_{k,i} \\ &= \mathbb{E}\left[a_{i,i}|\hat{a}_{i,i}\right] q_i + \left(a_{i,i} - \mathbb{E}\left[a_{i,i}|\hat{a}_{i,i}\right]\right) q_i + Z_{k,i}, \end{aligned} \tag{10}$$

where

$$Z_{k,i} = \sum_{j\neq i} a_{i,j} q_j + \boldsymbol{h}_i^T \left(\bar{\boldsymbol{w}}_k z + \boldsymbol{w}\right) + n_i. \tag{11}$$

$\mathbb{E}\left[a_{i,i}|\hat{a}_{i,i}\right] q_i$ is the desired information signal received through a deterministic precoded channel $\mathbb{E}\left[a_{i,i}|\hat{a}_{i,i}\right]$, while $\left(a_{i,i} - \mathbb{E}\left[a_{i,i}|\hat{a}_{i,i}\right]\right) q_i$ is the desired information signal received through a non-deterministic precoded channel $a_{i,i} - \mathbb{E}\left[a_{i,i}|\hat{a}_{i,i}\right]$. $\mathbb{E}\left[a_{i,i}|\hat{a}_{i,i}\right] q_i$ and $\left(a_{i,i} - \mathbb{E}\left[a_{i,i}|\hat{a}_{i,i}\right]\right) q_i$ are statistically dependent. $Z_{k,i}$ is the equivalent noise[6] which accounts for inter user interference, energy signal interference and the thermal noise. Referring to (9), we can see that $a_{i,i}$ is explicitly decoupled and therefore $a_{i,i}$ and $\tilde{a}_{i,i}$ are uncorrelated and statistically independent. Since $\hat{a}_{i,i}$ is deterministic at IU$_i$, then

$$\begin{aligned} &\mathbb{E}\left[a_{i,i}|\hat{a}_{i,i}\right] \\ &= \mathbb{E}\left[\hat{a}_{i,i}|\hat{a}_{i,i}\right] - \mathbb{E}\left[\tilde{a}_{i,i}|\hat{a}_{i,i}\right] = \hat{a}_{i,i} - \mathbb{E}\left[\tilde{a}_{i,i}\right] = \hat{a}_{i,i}, \end{aligned} \tag{12a}$$

$$a_{i,i} - \mathbb{E}\left[a_{i,i}|\hat{a}_{i,i}\right] = \tilde{a}_{i,i}, \tag{12b}$$

where $\mathbb{E}\left[\hat{a}_{i,i}|\hat{a}_{i,i}\right] = \hat{a}_{i,i}$ follows as an expectation over a deterministic value; $\mathbb{E}\left[\tilde{a}_{i,i}|\hat{a}_{i,i}\right] = \mathbb{E}\left[\tilde{a}_{i,i}\right]$ follows from the statistical independence between $\tilde{a}_{i,i}$ and $\hat{a}_{i,i}$; and $\mathbb{E}\left[\tilde{a}_{i,i}\right] = 0$ follows since $\mathbb{E}\left[\boldsymbol{n}_i \boldsymbol{\psi}_{d_i}^*\right] = 0$. Using the results in [25, Theorem 1] and in [26], the downlink information rate at the attacked user IU$_k$, $\underline{R}_k$ (given in (16) in Theorem 1) is achievable and forms a lower bound on the ergodic information rate R_k [26, (22)]

$$R_k = \mathbb{E}\left[\log_2\left(1 + \text{SINR}_k\right)\right], \tag{13}$$

where

$$\begin{aligned} \text{SINR}_k &= \frac{\left|\hat{a}_{k,k}\right|^2}{\mathbb{E}\left[\left|a_{k,k} - \mathbb{E}\left[a_{k,k}|\hat{a}_{k,k}\right]\right|^2\right] + \mathbb{E}\left[\left|Z_{k,k}\right|^2\right]} \\ &= \frac{\left|\hat{a}_{k,k}\right|^2}{\text{var}\left(\tilde{a}_{k,k}\right) + \text{var}\left(Z_{k,k}\right)}. \end{aligned} \tag{14}$$

Theorem 1: For $N \to \infty$, the value of SINR_k is tightly lower bounded by a deterministic value $\underline{\text{SINR}}_k \overset{N\to\infty}{<} \text{SINR}_k$, which is given by

$$\underline{\text{SINR}}_k = \frac{\tau^2 P_I c_k^2}{\sum\limits_{j\neq k} c_{k,j} + \tau^2 P_I \bar{c}_k^2 + \bar{c}_k^{(1)} + \tilde{c}_k + \sigma_n^2 \frac{\tau_d+1}{\tau_d}}, \tag{15}$$

[6]$Z_{k,i}$ is considered as an equivalent noise since $Z_{k,i}$ and $\mathbb{E}\left[a_{i,i}|\hat{a}_{i,i}\right] q_i$ are independent and that follows since $\{q_j\}$, z, n_i and $\boldsymbol{w}$ are statistically independent.

where

$$c_k = \boldsymbol{p}_k^T \text{diag}\left(\boldsymbol{\Gamma}_k \boldsymbol{C}_k\right),\ c_{k,j} = \boldsymbol{p}_j^T \boldsymbol{\Gamma}_k \boldsymbol{R}_j \boldsymbol{p}_j,\ \tilde{c}_k = \boldsymbol{p}^T \boldsymbol{\Gamma}_k \boldsymbol{R}\, \boldsymbol{p},$$
$$\bar{c}_k = \bar{\boldsymbol{p}}^T \text{diag}\left(\boldsymbol{\Gamma}_k \boldsymbol{C}_k\right),\ \bar{c}_k^{(1)} = \bar{\boldsymbol{p}}^T \boldsymbol{\Gamma}_k \boldsymbol{R}_k^{(1)} \bar{\boldsymbol{p}},\ \text{and}$$
$$\boldsymbol{R}_k^{(1)} = \bar{\boldsymbol{R}}_k - \tau^2 P_I \boldsymbol{C}_k^2 \boldsymbol{\Gamma}_k.$$

Since $\underline{\text{SINR}}_k$ is deterministic (independent of the small-fading randomness, $\mathbb{E}[\underline{\text{SINR}}_k] = \underline{\text{SINR}}_k$), and based on (13) and (15), $\underline{R}_k = \log_2(1 + \underline{\text{SINR}}_k)$ is a tight lower bound on the ergodic rate of the attacked user IU_k, and known at the CPU, i.e.,

$$\underline{R}_k = \log_2\left(1 + \underline{\text{SINR}}_k\right) \overset{N\to\infty}{<} R_k. \tag{16}$$

Proof: See Appendix A. ∎

B. Upper Bound on the EH Ergodic Rate

The received signal at the eavesdropping antenna of the EH, y_{E_k}, given in (6) can be recast as follows

$$y_{E_k} = b_k q_k + \sum_{j\neq k} b_j q_j + \hat{b}_k z + b + \bar{n}, \tag{17}$$

where

$$b_j = \boldsymbol{g}_E^T \boldsymbol{w}_j,\ \hat{b}_k = \boldsymbol{g}_E^T \bar{\boldsymbol{w}}_k,\ b = \boldsymbol{g}_E^T \boldsymbol{w}.$$

In the following, we assume the worst-case scenario in which the EH has full knowledge of its own channel vectors, $\boldsymbol{g}_E$ and $\boldsymbol{g}$; and the beamforming vectors $\{\boldsymbol{w}_i\}$. With this worst-case assumption, an upper bound on the ergodic information rate at the EH is given in the following theorem.

Theorem 2: With a worst-case scenario assumption that the EH has full knowledge of its own channel and the beamforming vectors of the IUs, the EH is capable of cancelling the inter-user interference [27, Chapter 8]. Since the information, $\{q_i\}$, the AN signal, z, and the energy signal, $\boldsymbol{w}$, are statistically independent, we have the following upper bound, $\overline{R}_{E_k}$, on the ergodic rate of the EH intending to eavesdrop IU_k, R_{E_k}, given by

$$\overline{R}_{E_k} = \log_2\left(1 + \mathbb{E}\left[\text{SINR}_{E_k}\right]\right) \geq R_{E_k} = \mathbb{E}\left[\log_2\left(1 + \text{SINR}_{E_k}\right)\right], \tag{18}$$

for which

$$\mathbb{E}\left[\text{SINR}_{E_k} = \frac{|b_k|^2}{|\hat{b}_k|^2 + |b|^2 + \sigma_n^2}\right] \overset{N\to\infty}{\to}$$
$$\frac{\mathbb{E}\left[|b_k|^2\right]}{\mathbb{E}\left[|\hat{b}_k|^2 + |b|^2 + \sigma_n^2\right]} = \frac{\tau^2 \phi P_E d_k^2 + d_k^{(1)}}{\tau^2 \phi P_E \bar{d}_k^2 + \bar{d}_k^{(1)} + d + \sigma_n^2}, \tag{19}$$

where

$$d_k = \boldsymbol{p}_k^T \text{diag}\left(\boldsymbol{\Gamma}\boldsymbol{C}_k\right),\ d_k^{(1)} = \boldsymbol{p}_k^T \boldsymbol{\Gamma} \boldsymbol{R}_k^{(2)} \boldsymbol{p}_k,\ d = \boldsymbol{p}^T \boldsymbol{\Gamma} \boldsymbol{R}\, \boldsymbol{p},\ \bar{d}_k =$$
$$\bar{\boldsymbol{p}}^T \text{diag}\left(\boldsymbol{\Gamma}\boldsymbol{C}_k\right),\ \bar{d}_k^{(1)} = \bar{\boldsymbol{p}}^T \boldsymbol{\Gamma} \boldsymbol{R}_k^{(2)} \bar{\boldsymbol{p}},\ \text{and}$$
$$\boldsymbol{R}_k^{(2)} = \bar{\boldsymbol{R}}_k - \tau^2 \phi P_E \boldsymbol{C}_k^2 \boldsymbol{\Gamma}.$$

Proof: See Appendix A. ∎

Such a worst-case scenario is commonly employed by much of the current research to guarantee maximum information security [17], [28]. Ensuring the confidentiality of the information for the worst-case scenario design ensures confidentiality for more optimistic scenarios.

C. Lower Bound on the Ergodic Secrecy Rate of IU_k

Using the lower bound and the upper bound on the information rates at the attacked user IU_k and the EH given in (16) and (18), we assess the secrecy of information at IU_k in terms of ESR, which has the following lower bound

$$R_{S_k} \overset{N\to\infty}{\to} \left[\underline{R}_k - \overline{R}_{E_k}\right]^+. \tag{20}$$

D. Average Harvested Energy at the EH

The EH relies on the dual functionality of its antennas to harvest energy and eavesdrop information simultaneously. The whole signal received via the legitimate antenna is devoted for energy harvesting, while the signal received via the illegitimate antenna is used for information decoding. However, since the CPU blames the EH for the active attack, the received signals via both antennas are accounted by the CPU for energy harvesting. The AHE by the EH intending to eavesdrop IU_k is[7]

$$E_k = \zeta\, \mathbb{E}\Bigg[|b_k|^2 + \sum_{j\neq k} |b_j|^2 + \left|\hat{b}_k\right|^2 + |b|^2 + \sum_j \left|\tilde{b}_j\right|^2 + \left|\tilde{\hat{b}}_k\right|^2$$
$$+ \left|\tilde{b}\right|^2 \Bigg] = \zeta \Bigg[\tau^2 \phi P_E d_k^2 + d_k^{(1)} + \sum_{j\neq k} d_{k,j} + \tau^2 \phi P_E \bar{d}_k^2 + \bar{d}_k^{(1)}$$
$$+ d + \sum_j d_{k,j} + \tilde{d}_k + \tau^2 (1-\phi) P_E \tilde{d}^2 + \tau \sigma_n^2 \tilde{d}^{(1)} \Bigg], \tag{21}$$

where

$$\tilde{b}_j = \boldsymbol{g}^T \boldsymbol{w}_j,\ \tilde{\hat{b}}_k = \boldsymbol{g}^T \bar{\boldsymbol{w}}_k,\ \tilde{b} = \boldsymbol{g}^T \boldsymbol{w},\ d_{k,j} = \boldsymbol{p}_j^T \boldsymbol{\Gamma} \boldsymbol{R}_j \boldsymbol{p}_j,$$
$$\tilde{d}_k = \bar{\boldsymbol{p}}^T \boldsymbol{\Gamma} \bar{\boldsymbol{R}}_k\, \bar{\boldsymbol{p}},\ \tilde{d} = \boldsymbol{p}^T \text{diag}\left(\boldsymbol{\Gamma}\boldsymbol{C}\right),\ \text{and}\ \tilde{d}^{(1)} = \boldsymbol{p}^T \boldsymbol{\Gamma} \boldsymbol{C}^2 \boldsymbol{p}.$$

IV. Power Control of Downlink Transmission

A. Problem Formulation

In our system, a single AP, AP_j, transmits a set of $M+2$ different types of signals, $\{\{[\boldsymbol{w}_i]_j q_i\}_i,\ [\bar{\boldsymbol{w}}_k]_j z,\ [\boldsymbol{w}]_j\}$. With the random geometric distribution of the APs with respect to the IUs and the EH, the power control in the cell-free MIMO system has an advantage over the conventional MIMO that different users have different subsets of dominant serving APs. In the long-term, the CPU can achieve a fair and secured SWIPT transmission towards the IUs and the EH by balancing the average levels of transmit powers at the APs within the power limits of each AP. The power control aims to maximize the worst-case ESR, $\min_k R_{S_k}$, with a constraint

[7] Detailed derivation of the results in (21) are in Appendix A.

on the minimum AHE requirement of the legitimate EH. Therefore, our constrained problem is

$$\begin{aligned}
&\underset{\{\boldsymbol{p}_i\},\ \bar{\boldsymbol{p}},\ \boldsymbol{p}}{\text{maximize}} \quad \min_k R_{S_k} \\
&\text{subject to} \quad E_k \geq \bar{E},\ \forall k, && \text{(22a)} \\
&\left[\sum_{i=1}^{M} \mathbb{E}[\boldsymbol{w}_i \boldsymbol{w}_i^H] + \mathbb{E}[\bar{\boldsymbol{w}}_k \bar{\boldsymbol{w}}_k^H] + \mathbb{E}[\boldsymbol{w}\boldsymbol{w}^H]\right]_{j,j} \leq P_t, \\
&\forall j,\ \forall k, && \text{(22b)}
\end{aligned}$$

where P_t is the available power budget at each AP. The constraint (22b) guarantees the average power consumption at each AP is within the limit, P_t. Problem (22) is non-convex since the objective function is a logarithm of multiplicative fractional functions. Without loss of generality, we assume that (22) is always feasible and focus on solving it. We use the exponential variable substitution method used in [29] and [30] to transform the logarithmic objective function of (22) into an equivalent linear function. By using the properties of logarithmic and exponential functions, the objective function of (22) can be expressed as $\log_e 2 \ln(e^{u_k - s_k} e^{v_k - t_k})$ where

$$e^{u_k} = \tau^2 P_I c_k^2 + \sum_{j \neq k} c_{k,j} + \tau^2 P_I \bar{c}_k^2 + \bar{c}_k^{(1)} + \tilde{c}_k + \sigma_n^2 \frac{\tau_d + 1}{\tau_d} \tag{23a}$$

$$e^{s_k} = \sum_{j \neq k} c_{k,j} + \tau^2 P_I \bar{c}_k^2 + \bar{c}_k^{(1)} + \tilde{c}_k + \sigma_n^2 \frac{\tau_d + 1}{\tau_d} \tag{23b}$$

$$e^{t_k} = \tau^2 \phi P_E d_k^2 + d_k^{(1)} + \tau^2 \phi P_E \bar{d}_k^2 + \bar{d}_k^{(1)} + d + \sigma_n^2 \tag{23c}$$

$$e^{v_k} = \tau^2 \phi P_E \bar{d}_k^2 + \bar{d}_k^{(1)} + d + \sigma_n^2. \tag{23d}$$

Since the logarithmic functions are monotonically increasing in their arguments, then (22) can be recast as

$$\begin{aligned}
&\underset{\{\boldsymbol{p}_i\},\ \bar{\boldsymbol{p}},\ \boldsymbol{p}\{u_k,\ s_k,\ t_k,\ v_k\}}{\text{maximize}} \quad \min_k (u_k - s_k + v_k - t_k) \\
&\text{subject to} \\
&\tau^2 P_I c_k^2 + \sum_{j \neq k} c_{k,j} + \tau^2 P_I \bar{c}_k^2 + \bar{c}_k^{(1)} + \tilde{c}_k + \sigma_n^2 \frac{\tau_d + 1}{\tau_d} \geq e^{u_k},\ \forall\ k, && \text{(24a)} \\
&\sum_{j \neq k} c_{k,j} + \tau^2 P_I \bar{c}_k^2 + \bar{c}_k^{(1)} + \tilde{c}_k + \sigma_n^2 \frac{\tau_d + 1}{\tau_d} \\
&\leq e^{\bar{s}_k} (s_k - \bar{s}_k + 1),\ \forall\ k, && \text{(24b)} \\
&\tau^2 \phi P_E d_k^2 + d_k^{(1)} + \tau^2 \phi P_E \bar{d}_k^2 + \bar{d}_k^{(1)} + d + \sigma_n^2 \\
&\leq e^{\bar{t}_k} (t_k - \bar{t}_k + 1),\ \forall\ k, && \text{(24c)} \\
&\tau^2 \phi P_E \bar{d}_k^2 + \bar{d}_k^{(1)} + d + \sigma_n^2 \geq e^{v_k},\ \forall\ k, && \text{(24d)} \\
&\text{(22a), (22b).} && \text{(24e)}
\end{aligned}$$

Our new objective in (24) is monotonically increasing with $\min_k R_{S_k}$. The constraints (24a)–(24e) bound the slack variables $u_k,\ s_k,\ t_k,\ v_k$ of the objective function within their limits defined in (23a)–(23d). The exponential variables e^{s_k} and e^{t_k} are linearized as $e^{\bar{s}_k}(s_k - \bar{s}_k + 1)$ and $e^{\bar{t}_k}(t_k - \bar{t}_k + 1)$. $\bar{s}_k,\ \bar{t}_k$ are the initial values around which e^{s_k} and e^{t_k} are linearized.

The formulation in (24) is still non-convex since the right-hand sides of the constraints (24a)–(24e) contain expressions which are nonlinear in the optimization variables (the power control factors $\{\{\boldsymbol{p}_i\},\ \bar{\boldsymbol{p}},\ \boldsymbol{p}\}$), such as $c_k^2 = \left(\boldsymbol{p}_k^T \text{diag}\left(\boldsymbol{\Gamma}_k \boldsymbol{C}_k\right)\right)^2$. These nonlinearities arise from the per AP per user power control (specific for cell-free massive MIMO systems) where each AP has its own transmit power constraint. In comparison, these nonlinearities do not exist in the power control for the conventional (collocated) massive MIMO systems in which the constraint is on the total transmit power from all collocated antennas [11]. To deal with these nonlinearities, we introduce a new method of cooperative balancing of the transmit powers at the APs via relaxed SDP formulation which has been proven to be optimal as will be described in the next subsection.

B. SDP Formulation for Optimal Power Control

In this subsection, we reformulate the non-convex problem (24) into a relaxed SDP convex problem. To achieve this, the nonlinear expressions in the power control factors $\{\{\boldsymbol{p}_i\},\ \bar{\boldsymbol{p}},\ \boldsymbol{p}\}$ are represented as linear expressions in terms of new rank-one positive semidefinite matrix variables $\{\{\boldsymbol{P}_i = \boldsymbol{p}_i\ \boldsymbol{p}_i^H\},\ \bar{\boldsymbol{P}} = \bar{\boldsymbol{p}}\ \bar{\boldsymbol{p}}^H,\ \boldsymbol{P} = \boldsymbol{p}\ \boldsymbol{p}^H\}$. For instance, given that k is the index of the IU under attack, the expression of c_k^2 can be recast in an SDP form as

$$\begin{aligned}
c_k^2 &= \left(\boldsymbol{p}_k^T \text{diag}\left(\boldsymbol{\Gamma}_k \boldsymbol{C}_k\right)\right)^2 = \boldsymbol{p}_k^T \text{diag}\left(\boldsymbol{\Gamma}_k \boldsymbol{C}_k\right) \text{diag}\left(\boldsymbol{\Gamma}_k \boldsymbol{C}_k\right)^T \boldsymbol{p}_k \\
&= \text{tr}\left(\boldsymbol{p}_k \boldsymbol{p}_k^T \text{diag}\left(\boldsymbol{\Gamma}_k \boldsymbol{C}_k\right) \text{diag}\left(\boldsymbol{\Gamma}_k \boldsymbol{C}_k\right)^T\right) = \text{tr}\left(\boldsymbol{P}_k \boldsymbol{A}_k\right),
\end{aligned} \tag{25}$$

where $\boldsymbol{A}_k = \text{diag}(\boldsymbol{\Gamma}_k \boldsymbol{C}_k)\ \text{diag}(\boldsymbol{\Gamma}_k \boldsymbol{C}_k)^T$. In a comparable way, the rest of the expressions $\{c_{k,j},\ \bar{c}_k^2,\ \bar{c}_k^{(1)},\ \tilde{c}_k\}$, $\{d_k^2,\ d_k^{(1)},\ d,\ \bar{d}_k^2,\ \bar{d}_k^{(1)}\}$ and $\{d_{k,j},\ \tilde{d}_k,\ \tilde{d}^2,\ \tilde{d}^{(1)}\}$ in (24) can be transformed into linear expressions in terms of $\{\{\boldsymbol{P}_i\},\ \bar{\boldsymbol{P}},\ \boldsymbol{P}\}$. With these transformations, we can recast the non-convex problem in (24) into a convex relaxed[8] SDP formulation as in (26) at the top of the next page, where $\mathbb{S} = \{\{\boldsymbol{P}_i\},\ \bar{\boldsymbol{P}},\ \boldsymbol{P},\ \{u_k,\ s_k,\ t_k,\ v_k\}\}$ is the set of optimization variables and

$$\begin{aligned}
&\boldsymbol{A}_{k,j} = \boldsymbol{\Gamma}_k \boldsymbol{R}_j,\ \bar{\boldsymbol{A}}_k = \boldsymbol{\Gamma}_k \boldsymbol{R}_k^{(1)},\ \tilde{\boldsymbol{A}}_k = \boldsymbol{\Gamma}_k \boldsymbol{R},\ \bar{\boldsymbol{B}}_k = \boldsymbol{\Gamma} \boldsymbol{R}_k^{(2)} \\
&\boldsymbol{B}_k = \text{diag}\left(\boldsymbol{\Gamma} \boldsymbol{C}_k\right) \text{diag}\left(\boldsymbol{\Gamma} \boldsymbol{C}_k\right)^H,\ \boldsymbol{B} = \boldsymbol{\Gamma} \boldsymbol{R},\ \tilde{\boldsymbol{B}} = \boldsymbol{\Gamma} \boldsymbol{R}_j \\
&\ddot{\boldsymbol{B}} = \text{diag}\left(\boldsymbol{\Gamma} \boldsymbol{C}\right) \text{diag}\left(\boldsymbol{\Gamma} \boldsymbol{C}\right)^H,\ \hat{\boldsymbol{B}} = \boldsymbol{\Gamma} \boldsymbol{C}^2,\ \text{and } \tilde{\boldsymbol{B}}_k = \boldsymbol{\Gamma} \bar{\boldsymbol{R}}_k.
\end{aligned}$$

The constraints (26e) and (26f) are an SDP recast of (22a) and (22b), respectively. The constraint (26f) is equivalent to (22b), where $\boldsymbol{D}_l \in \mathcal{R}^{N \times N}$ has zero entries except $[\boldsymbol{D}_l]_{l,l} = 1$. This equivalent representation in (26f) is required to facilitate the proof of Theorem 3 presented in Appendix A.

The formulation in (26) is convex and can be solved iteratively based on the following initial value update method: The initial values of the nth iteration $\{\bar{s}_k^{[n]}\}$ and $\{\bar{t}_k^{[n]}\}$ are updated by the optimized values of the $(n-1)$th preceding iteration $\{\ln(e^{\bar{s}_k^{[n-1]}}(s_k^{[n-1]} - \bar{s}_k^{[n-1]} + 1))\}$ and $\{\ln(e^{\bar{t}_k^{[n-1]}}(t_k^{[n-1]} - \bar{t}_k^{[n-1]} + 1))\}$, respectively. The iterations continue until the errors $\{|\bar{s}_k^{[n-1]} - \bar{s}_k^{[n]}|\}$ and $\{|\bar{t}_k^{[n-1]} - \bar{t}_k^{[n]}|\}$ converge to a certain small tolerance.

[8]The formulation in (26) does not impose any constraints on the rank of $\{\{\boldsymbol{P}_i\},\ \bar{\boldsymbol{P}},\ \boldsymbol{P}\}$, i.e, $\{\text{rank}(\boldsymbol{P}_i)\},\ \text{rank}(\bar{\boldsymbol{P}}),\ \text{rank}(\boldsymbol{P}) \leq N$.

$$\underset{\mathbb{S}}{\text{maximize}} \qquad \min_k \left(u_k - s_k + v_k - t_k\right)$$

subject to

$$\tau^2 P_I \text{tr}\left(\boldsymbol{P}_k \boldsymbol{A}_k\right) + \sum_{j\neq k} \text{tr}\left(\boldsymbol{P}_j \boldsymbol{A}_{k,j}\right) + \tau^2 P_I \text{tr}\left(\bar{\boldsymbol{P}} \boldsymbol{A}_k\right) + \text{tr}\left(\bar{\boldsymbol{P}} \bar{\boldsymbol{A}}_k\right) + \text{tr}\left(\boldsymbol{P} \tilde{\boldsymbol{A}}_k\right) + \sigma_n^2 \frac{\tau_d + 1}{\tau_d} \geq e^{u_k}, \ \forall\ k, \tag{26a}$$

$$\sum_{j\neq k} \text{tr}\left(\boldsymbol{P}_j \boldsymbol{A}_{k,j}\right) + \tau^2 P_I \text{tr}\left(\bar{\boldsymbol{P}} \boldsymbol{A}_k\right) + \text{tr}\left(\bar{\boldsymbol{P}} \bar{\boldsymbol{A}}_k\right) + \text{tr}\left(\boldsymbol{P} \tilde{\boldsymbol{A}}_k\right) + \sigma_n^2 \frac{\tau_d + 1}{\tau_d} \leq e^{\bar{s}_k} \left(s_k - \bar{s}_k + 1\right), \ \forall\ k, \tag{26b}$$

$$\tau^2 \phi P_E \text{tr}\left(\boldsymbol{P}_k \boldsymbol{B}_k\right) + \text{tr}\left(\boldsymbol{P}_k \bar{\boldsymbol{B}}_k\right) + \tau^2 \phi P_E \text{tr}\left(\bar{\boldsymbol{P}} \boldsymbol{B}_k\right) + \text{tr}\left(\bar{\boldsymbol{P}} \bar{\boldsymbol{B}}_k\right) + \text{tr}\left(\boldsymbol{P}\boldsymbol{B}\right) + \sigma_n^2 \leq e^{\bar{t}_k} \left(t_k - \bar{t}_k + 1\right), \ \forall\ k, \tag{26c}$$

$$\tau^2 \phi P_E \text{tr}\left(\bar{\boldsymbol{P}} \boldsymbol{B}_k\right) + \text{tr}\left(\bar{\boldsymbol{P}} \bar{\boldsymbol{B}}_k\right) + \text{tr}\left(\boldsymbol{P}\boldsymbol{B}\right) + \sigma_n^2 \geq e^{v_k}, \ \forall\ k, \tag{26d}$$

$$\zeta \Bigg(\tau^2 \phi P_E \text{tr}\left(\boldsymbol{P}_k \boldsymbol{B}_k\right) + \text{tr}\left(\boldsymbol{P}_k \bar{\boldsymbol{B}}_k\right) + \sum_{j\neq k} \text{tr}\left(\boldsymbol{P}_j \tilde{\boldsymbol{B}}_j\right) + \tau^2 \phi P_E \text{tr}\left(\bar{\boldsymbol{P}} \boldsymbol{B}_k\right) + \text{tr}\left(\bar{\boldsymbol{P}} \bar{\boldsymbol{B}}_k\right) + \text{tr}\left(\boldsymbol{P}\boldsymbol{B}\right) + \sum_j \text{tr}\left(\boldsymbol{P}_j \tilde{\boldsymbol{B}}_j\right)$$
$$+ \text{tr}\left(\bar{\boldsymbol{P}} \tilde{\boldsymbol{B}}_k\right) + \tau^2 (1-\phi) P_E \text{tr}\left(\boldsymbol{P} \ddot{\boldsymbol{B}}\right) + \tau \sigma_n^2 \text{tr}\left(\boldsymbol{P} \hat{\boldsymbol{B}}\right) \Bigg) \geq \bar{E}, \ \forall\ k, \tag{26e}$$

$$\text{tr}\left(\boldsymbol{P}_k \boldsymbol{D}_l \bar{\boldsymbol{R}}_k\right) + \sum_{j\neq k} \text{tr}\left(\boldsymbol{P}_j \boldsymbol{D}_l \boldsymbol{R}_j\right) + \text{tr}\left(\bar{\boldsymbol{P}} \boldsymbol{D}_l \bar{\boldsymbol{R}}_k\right) + \text{tr}\left(\boldsymbol{P} \boldsymbol{D}_l \boldsymbol{R}\right) - P_t \leq 0, \ \forall\ l, \ \forall\ k, \tag{26f}$$

$$\{\boldsymbol{P}_k\}, \ \bar{\boldsymbol{P}}, \ \boldsymbol{P} \succeq 0. \tag{26g}$$

It can be shown that the complex-valued SDP problem (27) (which is equivalent to (26)) contains: $M+2$ semidefinite complex-valued $N \times N$ matrix variables, $5M+1$ real scalar variables, $6M+NM+2$ constraints on matrix variable of size $N \times N$, and M constraints on scalar variables. The complexity (in terms of number of complex operations) of obtaining a per iteration solution of (26) within accuracy ϵ is asymptotically upper bounded by $\mathcal{O}(M^4 N^{\frac{9}{2}} \log(\frac{1}{\epsilon}))$ [31]. This result assumes unstructured input data matrices. However, the optimization solver (such as SeDuMi employed by CVX software [32]) can exploit the structure of input data matrices – for example, the structure of single non-zero element matrices $\{\boldsymbol{D}_l\}$ – to reduce the computational complexity [31].

C. Global Optimality of the SDP Formulation

To investigate the optimality of the solution obtained by (26), let us rewrite (26) in the equivalent form in (27) by replacing the objective $\min_k \left(u_k - s_k + v_k - t_k\right)$ by a new slack variable π and K linear constraints as

$$\underset{\substack{\{\boldsymbol{P}_i\},\ \bar{\boldsymbol{P}},\ \boldsymbol{P} \\ \{\text{diag}([u_k,\ s_k,\ t_k,\ v_k])\},\ \pi}}{\text{maximize}} \qquad \pi$$

$$\text{subject to} \qquad \text{diag}([u_k,\ s_k,\ t_k,\ v_k]) - \pi \boldsymbol{I_4} \succeq 0, \ \forall k, \tag{27a}$$

$$\text{(26a)–(26g)}. \tag{27b}$$

By examining (27) with the first-order and the second-order conditions of convexity, we have

$$\frac{\partial \pi}{\partial \pi} = 1, \quad \text{and} \quad \frac{\partial^2 \pi}{\partial \pi^2} = 0. \tag{28}$$

This means that (26) is convex with an affine objective function. Since the constraints of (26) are differentiable and there are no constraints on the domain of the optimization variables $\{\boldsymbol{P}_i\}, \ \bar{\boldsymbol{P}}, \ \boldsymbol{P} \in \mathcal{S}^+, \ \{u_k, \ s_k, \ t_k, \ v_k\}, \ \pi \in \mathcal{R}$, then Slater's condition holds and the solution obtained by solving (26) is globally optimal subject to: 1) satisfying the rank requirement of $\{\boldsymbol{P}_i\}, \ \bar{\boldsymbol{P}}$ and $\boldsymbol{P}$; 2) and the convergence of the constraints (26b) and (26c) (which results in the convergence of the iterative problem (26)).

1) Rank-one Optimality: Generally, the optimality of the solutions obtained via SDP programming might require a rank higher than one. The rank requirement for the optimality of the solutions obtained by SDP problems has been investigated in [33, Lemma 3.1] which is quoted as:

Lemma 2: Suppose that the separable SDP (P1) and its dual (D1) are solvable. Then, problem (P1) always has an optimal solution $\{\boldsymbol{X}_1^\star, \ \ldots, \ \boldsymbol{X}_L^\star\}$ *such that* $\sum_{l=1}^{L} \text{rank}^2(\boldsymbol{X}_l^\star) \leq M$.

$\{\boldsymbol{X}_1, \ \ldots, \ \boldsymbol{X}_L\}$ in Lemma 2 are the semi-definite matrix variables of (P1), $\{\boldsymbol{X}_1^\star, \ \ldots, \ \boldsymbol{X}_L^\star\}$ are their optimal values and M (for Lemma 2 only) is the number of constraints. Nevertheless, for our problem (26), the obtained solution $\{\boldsymbol{P}_i^\star\}, \ \bar{\boldsymbol{P}}^\star$ and $\boldsymbol{P}^\star$ needs to satisfy the rank-one structure $\{\text{rank}(\boldsymbol{P}_i^\star)\}, \ \text{rank}(\bar{\boldsymbol{P}}^\star), \ \text{rank}(\boldsymbol{P}^\star) = 1$ which complies with the optimality condition given in Lemma 2. The compliance of $\{\boldsymbol{P}_i^\star\}, \ \bar{\boldsymbol{P}}^\star$ and $\boldsymbol{P}^\star$ with rank-one requirement is given in the following theorem.

Theorem 3: Given that $\mathbb{S}^\star = \{\{\boldsymbol{P}_i^\star\}, \ \bar{\boldsymbol{P}}^\star, \ \boldsymbol{P}^\star, \ \{u_k^\star, \ s_k^\star, \ t_k^\star, \ v_k^\star\}\}$ is the solution obtained by solving (26), then, the optimized power control factor matrices $\{\boldsymbol{P}_i^\star\}, \ \bar{\boldsymbol{P}}^\star, \ \boldsymbol{P}^\star$ always satisfy the rank-one constraint, i.e., $\{\text{rank}(\boldsymbol{P}_i^\star)\}, \ \text{rank}(\bar{\boldsymbol{P}}^\star), \ \text{rank}(\boldsymbol{P}^\star) = 1$.

Proof: See Appendix B. ■

2) Convergence of the Iterative Problem: Here, we prove that the iterative optimization (26) converges to a globally optimal value, and the objective value (which is monotonically increasing with $\min_k R_{S_k}$) is increasing with the iterations. To facilitate our proof, let us introduce the following results.

Lemma 3: For arbitrary real values of x and $\bar{x} \neq x$, the first order approximation $e^{\bar{x}} \left(x - \bar{x} + 1\right)$ is always an underestimate of e^x, i.e. $e^{\bar{x}} \left(x - \bar{x} + 1\right) \leq e^x, \ \forall\ \bar{x} < x, \ \bar{x} > x$. In addition, the successive first order approximations of e^x; $f^{[n]} =$

$e^{\bar{x}^{[n]}}\left(x-\bar{x}^{[n]}+1\right)$ and $f^{[n+1]} = e^{\bar{x}^{[n+1]}}\left(x-\bar{x}^{[n+1]}+1\right)$, $e^{\bar{x}^{[n+1]}} = f^{[n]}$; always satisfy $f^{[n+1]} > f^{[n]}$ for $\bar{x}^{[n]} \neq x$.

Proof: Due to space limitation, the proof of Lemma 3 is omitted here, however, it is provided in a longer version of this paper (please refer to Appendix C therein) [34]. ■

Without loss of generality, we assume that (26) is feasible in its first iteration. Since our problem is convex and Slater's condition holds (see (28) and the paragraph that follows), constraints (26b) and (26c) can strictly hold. With the first order linearization in (26b) and (26c), and according to Lemma 3, the constraints (26b) and (26c) are tighter than their original formulations in (24b) and (24c), i.e., the feasibility region of (24) is smaller than the feasibility region of (26) (and forms a subregion of it). Therefore, any non-converged solution is suboptimal.

According to Lemma 3, and since the constraints (26b) and (26c) are initialized in the nth iteration by the optimal values obtained at the $(n-1)$th preceding iteration such as $e^{\bar{s}_k^{[n]}} = e^{\bar{s}_k^{[n-1]}}(s_k^{\star[n-1]} - \bar{s}_k^{[n-1]}+1)$ and $e^{\bar{t}_k^{[n]}} = e^{\bar{t}_k^{[n-1]}}(t_k^{\star[n-1]} - \bar{t}_k^{[n-1]}+1)$, $\forall\ k$, the feasibility of the $(n-1)$th iteration will ensure the feasibility of the succeeding nth iteration. Furthermore, the feasibility region at the nth iteration is larger than the feasibility region at the $(n-1)$th iteration and contains it. This ensures that the optimized objective value is monotonically increasing with the successive iteration. Given that the constrained values in (26b) and (26c) are finitely bounded (since both constraints are linear and the power budget at every AP is finite, $\leq P_t$), therefore, it can be concluded that the increasing optimized objective value will certainly converge, let us say at the nth iteration, i.e.

$$e^{\bar{s}_k^{[n]}}\left(s_k^{\star[n]} - \bar{s}_k^{[n]} + 1\right) = e^{\bar{s}_k^{[n-1]}}\left(s_k^{\star[n-1]} - \bar{s}_k^{[n-1]} + 1\right). \tag{29}$$

By solving the updating method, $e^{\bar{s}_k^{[n]}} = e^{\bar{s}_k^{[n-1]}}(s_k^{\star[n-1]} - \bar{s}_k^{[n-1]} + 1)$ and (29), we have $s_k^{\star[n]} = \bar{s}_k^{[n]}$, and $e^{\bar{s}_k^{[n]}}(s_k^{\star[n]} - \bar{s}_k^{[n]} + 1) = e^{s_k^{\star[n]}}$. This indicates that constraint (26b) converges to its original nonlinearized form. Likewise, constraint (26c) converges to its original nonlinearized form.

V. Evaluations

In this section, we evaluate the asymptotic performance of our SWIPT cell-free massive MIMO system. The APs are randomly located on a two dimensional Euclidean area A_a based on an homogeneous PPP Φ_a with an intensity λ_a. The IUs and the EH are randomly located on a two dimensional Euclidean area A_u with the origins of A_a and A_u coincident (please refer to footnote 1 regarding this assumption). The large-scale fading coefficients $\{\gamma_{i,j},\ \gamma_j\}$ are modeled with the standard distance-based model as $\gamma_{i,j} \triangleq d_{i,j}^{-\alpha}\ 10^{\frac{\nu_{i,j}}{10}}$ and $\gamma_j \triangleq d_j^{-\alpha}\ 10^{\frac{\nu}{10}}$, where $d_{i,j}$ and d_j are the distances from IU$_i$ and the EH to AP$_j$, respectively. α is the pathloss exponent and $\nu,\ \nu_{i,j} \sim \mathcal{CN}(0,\sigma^2)$ are the shadow fading coefficients with standard deviation σ. All users experience independent shadow fading, i.e., $\nu_{i,j}$ and $\nu_{i,j}$s are independent random variables (RVs). P, P_E and P_t are the training power budget at every IU, the training power budget at the EH, and the transmit power budget at every AP, respectively. τ and ζ are the length of the training sequences and the energy harvesting efficiency at the EH, respectively. Unless otherwise stated, and for referencing convenience, the selected values of system parameters are: $A_a = 1 \times 1$ Km^2, $\lambda_a = 1.5 \times 10^{-4}\ m^{-2}$, $A_u = 300 \times 300$ m^2, $M = 3$, $\alpha = 2.5$, $\sigma = 8$ dB [35], P, $P_E = 1\ W$, $P_t = 500\ mW$, $\tau,\ \tau_d = 10$ and $\zeta = 0.5$ [36].

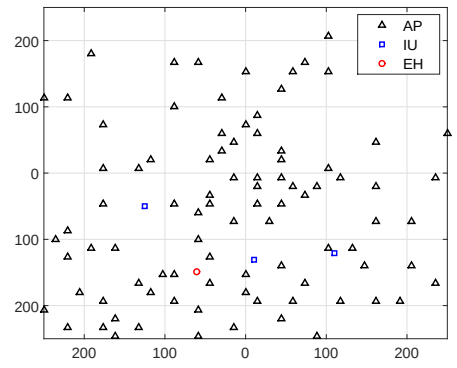

Fig. 2. AP-user deployment zoomed into the central 500×500 m^2 area, $N = 145$ and $M = 3$.

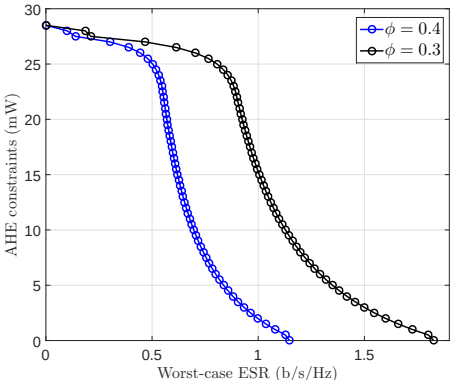

Fig. 3. E-R regions of colocated MIMO.

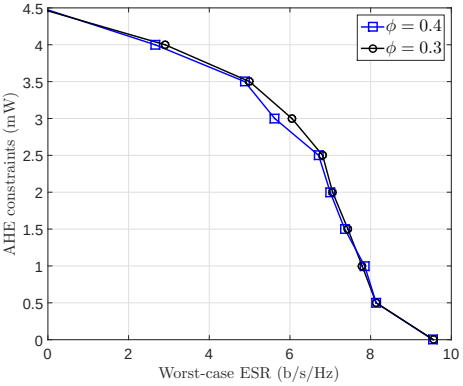

Fig. 4. E-R regions of cell-free MIMO.

Fig. 2 shows the AP-user deployment geometry of a realization in which the number of APs is $N = 145$ ($\mathbb{E}(N) =$

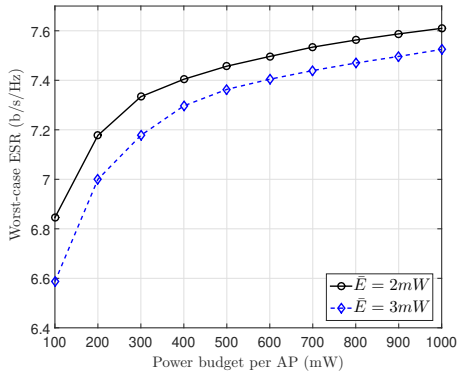

Fig. 5. ESR versus the power budgets per AP for $\phi = 0.5,\ \lambda_a = 10^{-4}m^{-2}$ and $\alpha = 2$.

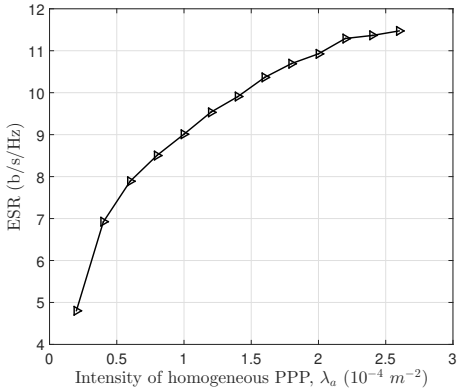

Fig. 6. ESR versus the intensity of homogeneous PPP, λ_a.

$\lambda_a A_a = 150$), $M = 3$ IUs and one EH zoomed into the central 500×500 m^2.

The SWIPT secrecy performance is presented by the E-R plot which relates the achievable worst-case ESR, $\min_k R_{S_k}$, to the constraint on the minimum AHE by the EH, $\bar{E}$. The larger the area under the E-R curve, the better the SWIPT performance. Our design analyses are made based on the asymptotic assumption $N \to \infty$, then, the system's performance can be examined for a realistic scenario of a large but finite number of APs.

In colocated MIMO systems, the user exhibits a constant average path-loss to all of the base station's (BS's) colocated antennas, and that average path-loss varies from one user to another based on the user's location. In contrast, in cell-free MIMO systems, the average path-loss of a given user varies from one AP to another. Intuitively, this property of randomly distributed APs is anticipated to increase the efficiency of power control in tackling the active eavesdropping. For fair comparisons between the performance of cell-free and colocated MIMO systems, a comparable model of a single-cell colocated massive MIMO system is derived such that: 1) the total number of colocated antennas at the BS is equal to the total number of APs, N; 2) the average value of a user's pathloss to the BS in colocated MIMO (all users experience equal pathlosses) is equal to the average value of the users' pathlosses in cell-free MIMO; 3) the total transmit power is equal for both systems, and the power limits at the colocated MIMO is per antenna; 4) the antennas of the BS are uncorrelated. Defining $\bar{\gamma}_i$ and $\bar{\gamma}$ as the pathlosses of IU$_i$ and the EH in the colocated MIMO system, respectively, we have $\bar{\gamma}_i = \sum_j \frac{\gamma_{i,j}}{N}$ and $\bar{\gamma} = \sum_j \frac{\gamma_j}{N}$. The downlink beamforming and power control of the colocated MIMO can be performed by the same methods used for cell-free MIMO.

Fig. 3 shows the E-R regions of the colocated MIMO system for two different values of active eavesdropping power corresponding to training power splitting factors $\phi = 0.3$ and $\phi = 0.4$. It can be noticed that there is a tradoff between the ESR and the constraint on the AHE. As the AHE constraint increases, more downlink transmission resources are optimized to satisfy the increase in AHE constraint at the expense of the ESR which tends to decrease. Also, there is a clear gap between the ESR performances at different levels of active eavesdropping powers. The larger the eavesdropping power the lower the ESR.

Fig. 4 shows the E-R regions of the cell-free MIMO system for the same values of active eavesdropping powers used for colocated MIMO system. By comparing Fig. 3 and Fig. 4, it can be noticed that the cell-free massive MIMO outperforms the colocated massive MIMO within the interval in which the harvested energy constraint is low and vice versa. The cell-free massive MIMO is also found to be more immune to the increase in the active eavesdropping power than the colocated massive MIMO. In colocated massive MIMO, all antennas contribute to the AHE by an equal average value which is not the case for the cell-free massive MIMO. Therefore, the colocated massive MIMO is more efficient at power transfer than the cell-free massive MIMO. The difference between channel gains of the IU and the EH in the cell-free system offers the optimizer more freedom to balance the tradeoff between the information, AN and the energy signal powers than in the case of the colocated massive MIMO system. That justifies the advantage of cell-free massive MIMO over the colocated massive MIMO in the feasible region (the low AHE constraint region).

Fig. 5 shows the variations in the ESR with respect to power budget per AP (all APs have equal power budgets). These results are obtained at different values of the constraint on the AHE, $\bar{E} = [2,\ 3]\ mW$. It can be observed that the ESR increases with the available power budgets at the APs, P_t. The rate of increase of the ESR with respect to P_t is larger at the lower range of P_t than at the upper range of P_t. This can be justified since the APs will not benefit effectively from the large budget because increasing the transmit power will increase interference among the APs and that reduces the advantage of the location diversity of APs.

Fig. 6 shows how the density of APs affects the secrecy performance. The achievable worst-case ESR is measured versus a set of practically large values of AP densities $\lambda_a = 10^{-4} \times [0.2,\ 0.4,\ ...,\ 2.6]\ m^{-1}$. The values of the worst-case ESR in Fig. 6 are obtained by Monte Carlo simulation averaged over 50 independent realizations of AP deployments, with $\bar{E} = 0$ and $\phi = 0.3$. As expected, as the AP density (which is directly proportional to $\mathbb{E}[N]$) increases, the worst-

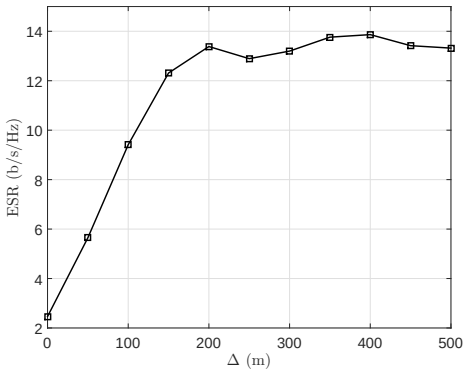

Fig. 7. ESR versus the separation between the IU and the EH for $\bar{E} = 0$, $\phi = 0.5$ and and $\alpha = 2$.

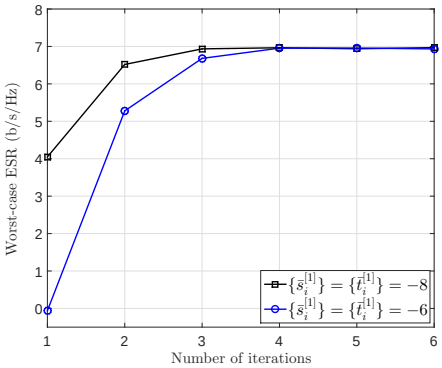

Fig. 8. Convergence speed of the iterative program in (26) for $\bar{E} = 2\ mW$ and $\phi = 0.4$.

case ESR increases.

The secrecy performance is affected by the relative location of the attacked IU with respect to the EH. Fig. 7 shows the ESR performance for the case where the system comprises one IU and one EH lying on the x-axis symmetrically around the origin of the APs' deployment given in Fig. 2. The results represent the achieved ESR for different separation distances between the IU and the EH, $\Delta = [0,\ 100,\ \ldots, 500]$. As the separation Δ increases, the ESR performance improves. This can be justified since as the separation increases, the AP subsets that dominantly serve the IU and the EH become more distinctive. Beyond a certain value of $\Delta > 200$, the achieved ESR starts to saturate since the dominant subsets of the APs that serve the IU and the EH remain unchanged, but the position of each user within its set varies. The value $\Delta = 0$ means that the IU and the EH are colocated, i.e., $\mathbf{\Gamma}_1 = \mathbf{\Gamma}$.

Fig. 8 shows the convergence speed of our iterative problem (26) at $\phi = 0.4$, $\bar{E} = 2\ mW$ and the initial values are selected arbitrarily as $\bar{s}_i^{[1]} = \bar{t}_i^{[1]} = [-8,\ -6]\ \forall i$. As discussed in Subsection IV-C2, the optimized objective value is increasing with iterations until convergence.

VI. Conclusions

In this paper, relaxed SDP programming has been proposed to optimize nonlinear power control of the downlink transmission in a SWIPT cell-free massive MIMO system in the presence of an information-untrusted dual-antenna active EH. The downlink SWIPT transmissions include: information, AN and energy signals beamformed towards the IUs, legitimate and illegitimate antennas of the EH, respectively. Analytic expressions for the AHE and a tight lower bound on the ESR were derived taking into account the IUs' knowledge attained by downlink effective precoded-channel training. It has been proved that the proposed SDP iterative problem can always achieve a converged rank-one globally optimal solution. A fair comparison between the proposed cell-free and the colocated massive MIMO systems showed that the cell-free massive MIMO outperformed the colocated massive MIMO over the interval in which the AHE constraint is low and vice versa. Also, cell-free massive MIMO was more immune to the increase in the active eavesdropping power than the colocated massive MIMO.

Considering the same problem under different eavesdropping models is an interesting topic for future work. Particularly, the eavesdropper might use the time switching or the power splitting receiving model for attacking one or multiple IUs for the purpose of information eavesdropping or energy harvesting, respectively.

Appendix A
Proofs of Lemma 1, Theorems 1 and 2

A. Proof of Lemma 1

Since the spectral radius of the diagonal matrices $\mathbf{\Gamma}_i$, $\mathbf{\Gamma}$ and $\sqrt{\mathbf{\Gamma}_i\mathbf{\Gamma}}$ are bounded [11, Lemma 2], then by expanding $\boldsymbol{y}_i^H\boldsymbol{y}_i$ followed by applying Corollary 1 in [37] we get

$$\boldsymbol{y}_i^H\boldsymbol{y}_i - \tau^2 P_I \mathrm{tr}\left(\mathbf{\Gamma}_i\right) - N\tau\sigma_n^2 \overset{N\to\infty}{\to} \delta_{ij}\ \tau^2\phi P_E \mathrm{tr}\left(\mathbf{\Gamma}\right), \qquad (30)$$

which satisfies the asymptotic convergence in (3). This concludes the proof.

B. Proof of Theorem 1

Before commencing our proof, let us introduce the following result.

Proposition 1: For a non-negative bounded RV $0 \le X_1 \le U$, U is a positive real value, and a symmetrical zero mean RV X_2. Knowing that the RV $Y = X_1 + X_2$ is non-negative, then Y is upper bounded as $Y \le 2U$.

Proof: The proof is presented through the following points:

(a) Given that Y is non-negative RV, then $P((Y = X_1 + X_2) < 0) = 0$ is always true.

(b) $P(U + X_2 < 0) = 0$ (i.e., $P(X_2 < -U) = 0$) is always true, since by contradiction $P(X_2 < -U) \neq 0$ can result in $X_2 < -U$ and therefore $X_1 + X_2 < 0$ (note that $X_1 \le U$ is given). This result contradicts the assumption of the non-negativeness of Y.

(c) Since the probability distribution of X_2 is symmetrical around zero (given assumption), and since we have proven in (b) that $P(X_2 < -U) = 0$, then by symmetry of distribution $P(X_2 > U) = 0$ is always true (otherwise

X_2 is not a symmetrical zero mean RV). The obtained result $P(X_2 > U) = 0$ implies that the RV X_2 is upper bounded as $X_2 \leq U$.

(d) From the given upper bound on X_1, $X_1 \leq U$, and the proved upper bound on X_2, $X_2 \leq U$, it can be concluded that $Y = X_1 + X_2$ is upper bounded as $Y \leq 2U$.

This concludes the proof. ∎

Let IU_k be the attacked IU. Based on (2), (5a), (7) and (9) we have

$$|\hat{a}_{k,k}|^2 = \tau^2 P_I \left| \bar{\boldsymbol{h}}_k^H \boldsymbol{\Gamma}_k^{\frac{1}{2}} \text{diag}\left(\boldsymbol{p}_k\right) \boldsymbol{C}_k \boldsymbol{\Gamma}_k^{\frac{1}{2}} \bar{\boldsymbol{h}}_k \right|^2 + \left| \bar{\boldsymbol{h}}_k^H \boldsymbol{\Gamma}_k^{\frac{1}{2}} \text{diag}\left(\boldsymbol{p}_k\right) \boldsymbol{C}_k \tilde{\boldsymbol{h}}_k \right|^2 + \left| \frac{\boldsymbol{n}_k \boldsymbol{\psi}_{d_k}^*}{\tau_d} \right|^2, \tag{31}$$

where $\tilde{\boldsymbol{h}}_k = \hat{\boldsymbol{h}}_k - \tau\sqrt{P_I}\boldsymbol{C}_k \boldsymbol{h}_k = \tau\sqrt{\phi P_E}\ \boldsymbol{g}_E + \boldsymbol{N}\boldsymbol{\psi}_k^*$, and the entries of $\tilde{\boldsymbol{h}}_k$, $\boldsymbol{h}_k$ and $\boldsymbol{n}_k$ are statistically independent. Using Corollary 1 in [37] and Lemma 2 in [11], the first term in (31) asymptotically converges to the deterministic value

$$\begin{aligned} \Delta_1 &= \tau^2 P_I \text{tr}^2(\boldsymbol{\Gamma}_k \text{diag}(\boldsymbol{p}_k)\boldsymbol{C}_k) \\ &= \tau^2 P_I \left(\boldsymbol{p}_k^T \text{diag}(\boldsymbol{\Gamma}_k \boldsymbol{C}_k)\right)^2 = \tau^2 P_I \text{tr}\left(\boldsymbol{P}_k \boldsymbol{A}_k\right) = \tau^2 P_I c_k^2 = \\ &\tau^2 P_I \Big(\sum_j \gamma_{k,j}^2 \bar{c}_{k,j}^2 p_{k,j} + \sum_{\mathbb{I}} \gamma_{k,j}\gamma_{k,m} \bar{c}_{k,j}\bar{c}_{k,m}\sqrt{p_{k,j}p_{k,m}} \Big), \end{aligned} \tag{32}$$

where $\mathbb{I} = \{\{k,j\}_j \times \{k,m\}_m | \{k,j\} \neq \{k,m\}\}$ and $\bar{c}_{k,j} = [\boldsymbol{C}_k]_{j,j}$. With the assumption that the noise variance $\sigma_n^2 \ll \tau\phi P_E$, we can approximate the sum of the second and the third terms in (31) as $\Delta_2 = \tau^2 \phi P_E |\bar{\boldsymbol{h}}_k^H \boldsymbol{\Gamma}_k^{\frac{1}{2}} \text{diag}\left(\boldsymbol{p}_k\right) \boldsymbol{C}_k \boldsymbol{g}_E|^2$, which is equivalent to

$$\begin{aligned} \Delta_2 = &\tau^2 \phi P_E \Big(\sum_{j=1}^{N} \gamma_{k,j}\gamma_j \bar{c}_{k,j}^2 p_{k,j}\ \kappa_j + \\ &\sum_{\mathbb{I}} \sqrt{\gamma_{k,j}\gamma_j\gamma_{k,m}\gamma_m}\bar{c}_{k,j}\bar{c}_{k,m}\sqrt{p_{k,j}p_{k,m}}\ \kappa_{j,m} \Big), \end{aligned} \tag{33}$$

where $\kappa_j = |\hat{h}_{k,j}\hat{g}_{E_j}|^2$ (equivalent to the product of two independent exponential RVs of parameter 1) is a non-negative random variable with the mean value $\mathbb{E}[\kappa_j] = 1$. $\kappa_{j,m} = \hat{h}_{k,j}\hat{g}_{E_j}\hat{h}_{k,m}\hat{g}_{E_m}$, $j \neq m$, is a zero mean RV with a symmetric distribution [38], [39]. Since Δ_2 is always positive, i.e., $P(\Delta_2 < 0) = 0$, then, by applying Theorem A in [40] (which defines an upper bound on the sum of non-negative RVs) and Proposition 1, Δ_2 is upper bounded by a deterministic value as

$$\Delta_2 \leq \overline{\Delta}_2 = 4e\tau^2 \phi P_E \sum_{j=1}^{N} \gamma_{k,j}\gamma_j \bar{c}_{k,j}^2 p_{k,j}. \tag{34}$$

Given that the additive terms that constitute Δ_1 in (32) and the upper bound of Δ_2, $\overline{\Delta}_2$, in (34) are of a finite order of magnitude, then, asymptotically, we have $\Delta_1 \overset{N\to\infty}{\to} \mathcal{O}\left(N^2\right)$ and $\overline{\Delta}_2 \overset{N\to\infty}{\to} \mathcal{O}\left(N\right)$. Therefore, as $N \to \infty$, Δ_1 and Δ_2 differ by $\mathcal{O}\left(N\right)$ order of magnitude which implies that the bound $|\hat{a}_{k,k}|^2 \geq \Delta_1 = \tau^2 P_I \text{tr}\left(\boldsymbol{P}_k \boldsymbol{A}_k\right)$ is tight. Based on this result, (14), (15), and since SINR_k and $\underline{\text{SINR}}_k$ share the same denominator, then $\text{SINR}_k > \underline{\text{SINR}}_k$ in (15) is of the same degree of tightness. To validate the tightness of $\text{SINR}_k \overset{N\to\infty}{>} \underline{\text{SINR}}_k$ numerically, Table III presents the values of Δ_1, $\overline{\Delta}_2$ and $\frac{\Delta_1}{\overline{\Delta}_2}$ for different realizations of $\{\boldsymbol{\Gamma}_i\}$ and $\boldsymbol{\Gamma}$ at a large average value of $N = 100$, and at $\bar{E} = 5\ mW$. The optimized values of $\{\boldsymbol{P}_i\}$, $\bar{\boldsymbol{P}}$ and $\boldsymbol{P}$ used to obtain the values of Δ_1 are used to calculate corresponding value of $\overline{\Delta}_2$. The obtained results validate our analysis.

TABLE I. RELATIVE VALUES OF Δ_1 AND $\overline{\Delta}_2$

Realization	1st	2nd	3rd	4th
Δ_1	9.8×10^{-3}	7.3×10^{-3}	1.6×10^{-2}	4.6×10^{-3}
$\overline{\Delta}_2$	6.9×10^{-5}	1.1×10^{-4}	3.8×10^{-5}	1.2×10^{-4}
$\frac{\Delta_1}{\overline{\Delta}_2}$	1.4×10^2	0.65×10^2	4.1×10^2	0.3×10^2

The values of $\text{var}(Z_{k,k}) = \sum_{j\neq k} c_{k,j} + \tau^2 P_I \bar{c}_k^2 + \bar{c}_k^{(1)} + \tilde{c}_k$ and $\text{var}(\tilde{a}_{k,k}) = \sigma_n^2 \frac{\tau_d + 1}{\tau_d}$ (as in (14)-(15)) can be derived in a similar way to that used for deriving the value of $c_k^2 = \text{tr}\left(\boldsymbol{P}_k \boldsymbol{A}_k\right)$ in (32) and (31). Therefore, due to space limitation, their analyses are omitted here, however, they can be found in a longer version of this paper (please refer to Appendix A therein) [34]. This concludes the proof.

C. Proof of Theorem 2

Based on the assumption that the EH has a full knowledge of the IUs' beamforming vectors and its own channel, the EH is capable of cancelling the inter-user interference [27]. Furthermore, the information, AN and energy signals; $\{q_i\}$, z and $\boldsymbol{w}$; are statistically independent. Therefore, based on the concavity of the logarithmic function, applying Jensen's inequality (which has been proven to be tight and suitable for characterizing the performance of massive MIMO systems [41]) will result in the following upper bound on the ergodic rate at the EH

$$\overline{R}_{E_k} = \log_2\left(1 + \mathbb{E}\left[\text{SINR}_{E_k}\right]\right) > \mathbb{E}\left[\log_2\left(1 + \text{SINR}_{E_k}\right)\right], \tag{35}$$

where SINR_{E_k} is the SINR at the EH when attacking IU_k. As defined in (19), $\text{SINR}_{E_k} = \frac{X_k}{Y_k}$, $X_k = \mathbb{E}[|\boldsymbol{g}_E^T \boldsymbol{w}_k q_k|^2] = |b_k|^2$ and $Y_k = \mathbb{E}[|\boldsymbol{g}_E^T(\bar{\boldsymbol{w}}_k z + \boldsymbol{w}) + \bar{n}|^2] = |\hat{b}_k|^2 + |b|^2 + \sigma_n^2$. Using the multivariate Taylor expansion, $\mathbb{E}[\text{SINR}_{E_k}]$ can be expanded as [42]

$$\begin{aligned} \mathbb{E}\left[\text{SINR}_{E_k}\right] &= \mathbb{E}\left[\frac{X_k}{Y_k}\right] \\ &= \frac{\mathbb{E}[X_k]}{\mathbb{E}[Y_k]} - \frac{\text{cov}(X_k, Y_k)}{(\mathbb{E}[Y_k])^2} + \frac{\text{var}(Y_k)}{(\mathbb{E}[Y_k])^2}\ \frac{\mathbb{E}[X_k]}{\mathbb{E}[Y_k]} + R. \end{aligned} \tag{36}$$

where $R = f(\text{var}(Y_k), \text{cov}(X_k, Y_k))$ is the remainder of the series expansion. We have

$$\begin{aligned} &\mathbb{E}[X_k] = \mathbb{E}[|b_k|^2] = \mathbb{E}[|\boldsymbol{g}_E^T \boldsymbol{w}_k|^2] \\ &= \mathbb{E}\left[\left|\boldsymbol{g}_E^T \text{diag}\left(\boldsymbol{p}_k\right)\left(\tau\sqrt{\phi P_E}\boldsymbol{C}_k \boldsymbol{g}_E^* + \tilde{\boldsymbol{h}}_k^{(2)}\right)\right|^2\right] = \tau^2 \phi P_E \\ &\mathbb{E}\left[\left|\bar{\boldsymbol{g}}_E^T \boldsymbol{\Gamma}^{\frac{1}{2}} \text{diag}\left(\boldsymbol{p}_k\right) \boldsymbol{C}_k \boldsymbol{\Gamma}^{\frac{1}{2}} \bar{\boldsymbol{g}}_E^*\right|^2\right] + \mathbb{E}\left[\left|\boldsymbol{g}_E^T \text{diag}\left(\boldsymbol{p}_k\right) \tilde{\boldsymbol{h}}_k^{(2)}\right|^2\right], \end{aligned} \tag{37}$$

where

$$\mathbb{E}\left[\left|\bar{\boldsymbol{g}}_E^T\boldsymbol{\Gamma}^{\frac{1}{2}}\text{diag}\left(\boldsymbol{p}_k\right)\boldsymbol{C}_k\boldsymbol{\Gamma}^{\frac{1}{2}}\bar{\boldsymbol{g}}_E^*\right|^2\right] = \left|\boldsymbol{p}_k^T\text{diag}\left(\boldsymbol{\Gamma}\boldsymbol{C}_k\right)\right|^2$$
$$= \text{tr}\left(\boldsymbol{P}_k\text{diag}\left(\boldsymbol{\Gamma}\boldsymbol{C}_k\right)\text{diag}\left(\boldsymbol{\Gamma}\boldsymbol{C}_k\right)^H\right) = \text{tr}\left(\boldsymbol{P}_k\boldsymbol{B}_k\right), \quad (38a)$$

$$\mathbb{E}\left[\left|\boldsymbol{g}_E^T\text{diag}\left(\boldsymbol{p}_k\right)\tilde{\boldsymbol{h}}_k^{(2)}\right|^2\right]$$
$$= \mathbb{E}\left[\bar{\boldsymbol{g}}_E^T\boldsymbol{\Gamma}^{\frac{1}{2}}\text{diag}\left(\boldsymbol{p}_k\right)\mathbb{E}\left[\tilde{\boldsymbol{h}}_k^{(2)}\tilde{\boldsymbol{h}}_k^{(2)^H}\right]\text{diag}\left(\boldsymbol{p}_k\right)\boldsymbol{\Gamma}^{\frac{1}{2}}\bar{\boldsymbol{g}}_E^*\right]$$
$$= \text{tr}\left(\boldsymbol{\Gamma}^{\frac{1}{2}}\text{diag}\left(\boldsymbol{p}_k\right)\boldsymbol{R}_k^{(2)}\text{diag}\left(\boldsymbol{p}_k\right)\boldsymbol{\Gamma}^{\frac{1}{2}}\right) = \text{tr}\left(\boldsymbol{p}_k^T\boldsymbol{\Gamma}\boldsymbol{R}_k^{(2)}\boldsymbol{p}_k\right)$$
$$= \text{tr}\left(\boldsymbol{P}_k\boldsymbol{\Gamma}\boldsymbol{R}_k^{(2)}\right) = \text{tr}\left(\boldsymbol{P}_k\bar{\boldsymbol{B}}_k\right), \quad (38b)$$

where $\tilde{\boldsymbol{h}}_k^{(2)} = \hat{\boldsymbol{h}}_k^* - \tau\sqrt{\phi P_E}\boldsymbol{C}_k\boldsymbol{g}_E^*$ and $\boldsymbol{R}_k^{(2)} = \mathbb{E}[\tilde{\boldsymbol{h}}_k^{(2)}\tilde{\boldsymbol{h}}_k^{(2)^H}] = \bar{\boldsymbol{R}}_k - \tau^2\phi P_E\boldsymbol{C}_k^2\boldsymbol{\Gamma}$. The third equality in (37) is obtained by substituting the value of $\boldsymbol{w}_k$ from (5a), (2a) and (2b). The fourth equality in (37) follows from the statistical independence between $\boldsymbol{g}_E$ and $\tilde{\boldsymbol{h}}_k^{(2)}$. The first equality in (38a) follows from applying Corollary 1 in [37] and the diagonality of the matrices $\boldsymbol{\Gamma}$, $\boldsymbol{C}_k$ and $\text{diag}\left(\boldsymbol{p}_k\right)$. In the first equality in (38b), the expectation is moved to $\tilde{\boldsymbol{h}}_k^{(2)}\tilde{\boldsymbol{h}}_k^{(2)^H}$ based on the statistical independence between $\bar{\boldsymbol{g}}_E$ and $\tilde{\boldsymbol{h}}_k^{(2)}$. The second equality in (38b) follows from applying Corollary 1 in [37]. The third and the fourth equalities in (38b) follow from the diagonality of the matrices $\boldsymbol{\Gamma}$, $\boldsymbol{R}_k^{(2)}$ and $\text{diag}\left(\boldsymbol{p}_k\right)$. By substituting (38a) and (38b) in (37), we get $\mathbb{E}[X_k] = \mathbb{E}[|b_k|^2] = \tau^2\phi P_E d_k^2 + d_k^{(1)}$, $d_k^2 = \text{tr}(\boldsymbol{P}_k\boldsymbol{B}_k)$ and $d_k^{(1)} = \text{tr}(\boldsymbol{P}_k\bar{\boldsymbol{B}}_k)$. The details of deriving the value of

$$\mathbb{E}\left[Y_k\right] = \mathbb{E}\left[|\hat{b}_k|^2 + |b|^2 + \sigma_n^2\right] = \tau^2\phi P_E\bar{d}_k^2 + \bar{d}_k^{(1)} + d + \sigma_n^2,$$

where

$$d = \text{tr}(\boldsymbol{P}\boldsymbol{B}),\ \bar{d}_k^2 = \text{tr}(\bar{\boldsymbol{P}}\boldsymbol{B}_k)\ \text{ and }\ \bar{d}_k^{(1)} = \text{tr}(\bar{\boldsymbol{P}}\bar{\boldsymbol{B}}_k),$$

(as presented in (19)) are similar to the analyses used to obtain the value of $\mathbb{E}[|b_k|^2]$ previously described. Therefore, due to space limitation, the analyses of obtaining $\mathbb{E}[Y_k]$ are omitted here, however, they can be found in a longer version of this paper (please refer to Appendix A therein) [34]. For $\text{var}(Y_k)$ we have

$$\text{var}(Y_k) = \mathbb{E}\left[|Y_k - \mathbb{E}[Y_k]|^2\right] = \mathbb{E}\left[\left|\left|\boldsymbol{g}_E^T\boldsymbol{w}\right|^2 - \text{tr}\left(\boldsymbol{P}\boldsymbol{B}\right)\right|^2\right]$$
$$+ \mathbb{E}\left[\left|\left|\boldsymbol{g}_E^T\bar{\boldsymbol{w}}_k\right|^2 - \tau^2\phi P_E\text{tr}\left(\bar{\boldsymbol{P}}\boldsymbol{B}_k\right) - \text{tr}\left(\bar{\boldsymbol{P}}\bar{\boldsymbol{B}}_k\right)\right|^2\right] + \sigma_n^2. \quad (39)$$

The second equality in (39) follows from substituting the value of Y_k, and the statistical independence between $\boldsymbol{w}$, $\bar{\boldsymbol{w}}_k$ and $\bar{n}$. The first and the second terms in (39) are as follows

$$\mathbb{E}\left[\left|\left|\boldsymbol{g}_E^T\boldsymbol{w}\right|^2 - \text{tr}\left(\boldsymbol{P}\boldsymbol{B}\right)\right|^2\right] = 2\text{tr}^2\left(\boldsymbol{P}\boldsymbol{B}\right) - \text{tr}\left(\left(\boldsymbol{P}\boldsymbol{B}\right)^{\circ 2}\right), \quad (40)$$

$$\mathbb{E}\left[\left|\left|\boldsymbol{g}_E^T\bar{\boldsymbol{w}}_k\right|^2 - \tau^2\phi P_E\text{tr}\left(\bar{\boldsymbol{P}}\boldsymbol{B}_k\right) - \text{tr}\left(\bar{\boldsymbol{P}}\bar{\boldsymbol{B}}_k\right)\right|^2\right]$$
$$= 2\ \text{tr}^2\left(\bar{\boldsymbol{P}}\bar{\boldsymbol{B}}_k\right) - \text{tr}\left(\left(\bar{\boldsymbol{P}}\bar{\boldsymbol{B}}_k\right)^{\circ 2}\right), \quad (41)$$

where $\circ$ denotes the Hadamard power operation and $\mathbb{I} = \{\{j\} \times \{m\}|\ j \neq m\}$. The detailed analyses of obtaining the results in (40) and (41) are provided in a longer version of this paper (please refer to Appendix A therein) [34].

Given that the entries of the matrix $\boldsymbol{B}_k$ have non-zero positive values, the matrices $\bar{\boldsymbol{B}}_k$ and $\boldsymbol{B}$ are diagonal, and the additive terms in $(\text{tr}(\bar{\boldsymbol{P}}\boldsymbol{B}_k) + \text{tr}(\bar{\boldsymbol{P}}\bar{\boldsymbol{B}}_k) + \text{tr}(\boldsymbol{P}\boldsymbol{B}))^2$ are of a finite order of magnitude; then, asymptotically, we have $(\mathbb{E}[Y_k])^2 \overset{N\to\infty}{\to} \mathcal{O}\left(N^4\right)$ and $\text{var}(Y_k) \overset{N\to\infty}{\to} \mathcal{O}\left(2N^2\right)$. This implies that $\frac{\text{var}(Y_k)}{(E[Y_k])^2} \overset{N\to\infty}{\to} 0$ and $R = f(\text{var}(Y_k), \text{cov}(X_k, Y_k)) \overset{N\to\infty}{\to} 0$. Based on (36) and this result, and since $\text{cov}(X_k, Y_k) = 0$ (follows from the statistical independence between X_k and Y_k), we have

$$\mathbb{E}\left[\text{SINR}_{E_k}\right] \overset{N\to\infty}{\to} \frac{\mathbb{E}[X_k]}{\mathbb{E}[Y_k]} = \frac{\tau^2\phi P_E d_k^2 + d_k^{(1)}}{d + \tau^2\phi P_E\bar{d}_k^2 + \bar{d}_k^{(1)} + \sigma_n^2}. \quad (42)$$

By substituting (42) in (35), we get (18)–(19). This concludes the proof.

D. Deriving the asymptotic value of AHE in (21)

The details of deriving the values that constitute $\bar{E}_k$ in (21) are similar to the analyses used to obtain the values of $\mathbb{E}[|b_k|^2]$ and $\tau^2 P_I c_k^2 = \tau^2 P_I\text{tr}\left(\boldsymbol{P}_k\boldsymbol{A}_k\right)$ previously described in (37)–(38b) and (32), respectively. Therefore, their detailed derivations are omitted. However, the detailed derivations can be found in a longer version of this paper (please refer to Appendix A therein) [34].

APPENDIX B
PROOF OF THEOREM 3

To prove that the optimal solution $\{\boldsymbol{P}_i^\star\}$, $\bar{\boldsymbol{P}}^\star$, $\boldsymbol{P}^\star$ obtained by solving (26) is always of unity rank, we exploit the boundedness property of the dual Lagrangian function to show that the optimal primal matrices $\{\boldsymbol{P}_i^\star\}$, $\bar{\boldsymbol{P}}^\star$, $\boldsymbol{P}^\star$ can satisfy the KKT conditions of optimality at one case in which $\{\text{rank}(\boldsymbol{P}_i^\star)\}$, $\text{rank}(\bar{\boldsymbol{P}}^\star)$, $\text{rank}(\boldsymbol{P}^\star) = 1$, and that has been validated by computer simulation. Before commencing our proof let us introduce the following Lemma.

Lemma 4: Let $\mathbb{L} = \{\{\lambda_{1_k}\},\ \ldots,\ \{\lambda_{7_k}\},\ \{\boldsymbol{F}_k\},\ \bar{\boldsymbol{F}},\ \boldsymbol{F}\}$ be the Lagrange multipliers of the constraints (27a), (26a)–(26f) and the constraints on $\{\boldsymbol{P}_k\}$, $\bar{\boldsymbol{P}}$ and $\boldsymbol{P}$ in (26g), respectively, with $\{\lambda_{j_k}\} \geq 0$, $\{\boldsymbol{F}_k\}$, $\bar{\boldsymbol{F}}$, $\boldsymbol{F} \succeq \boldsymbol{0}$. The existence of the Lagrangian function for problem (27) and the satisfaction of the KKT's stationarity and complementary slackness condition imply $\text{tr}(\boldsymbol{P}_k^\star\boldsymbol{F}_k^\star) = 0,\ \forall k$, where

$$\boldsymbol{F}_k^\star = -\lambda_{2_k}\tau^2 P_I\boldsymbol{A}_k + \boldsymbol{G}_k^\star, \quad (43)$$

$$\boldsymbol{G}_k^\star = -\sum_{j\neq k}\lambda_{2_j}^\star\boldsymbol{A}_{j,k} - \lambda_{6_k}^\star\zeta\left(\tau^2\phi P_E\boldsymbol{B}_k + \bar{\boldsymbol{B}}_k\right) - \lambda_{6_j}^\star\zeta$$
$$\left(\sum_{j\neq k}\tilde{\boldsymbol{B}}_k + \sum_j\tilde{\boldsymbol{B}}_k\right) + \sum_l\left(\lambda_{7_k}^\star\boldsymbol{D}_l\bar{\boldsymbol{R}}_k + \sum_{j\neq k}\lambda_{7_j}^\star\boldsymbol{D}_l\boldsymbol{R}_k\right). \quad (44)$$

Proof: Due to space limitation, the proof is omitted in this paper, however, it is provided in a longer version of this paper (please refer to the proof of Theorem 3 in Appendix B therein) [34]. ■

Let null $(\boldsymbol{F}_k^\star) = \boldsymbol{\Omega}_k = [\boldsymbol{\omega}_{k,1}, ..., \boldsymbol{\omega}_{k,N-\text{rank}(\boldsymbol{F}_k^\star)}]$ and null$(\boldsymbol{G}_k^\star) = \boldsymbol{\Psi}_k = [\boldsymbol{\psi}_{k,1}, ..., \boldsymbol{\psi}_{k,N-\text{rank}(\boldsymbol{G}_k^\star)}]$. By making use of the inequality of matrix sum [43, subsection 3.3.4] and (43) we have[9] $\text{rank}(\boldsymbol{F}_k^\star) \geq \text{rank}(\boldsymbol{G}_k^\star) - 1$. Based on this result, and since $\text{rank}(\boldsymbol{\Omega}_k) = N - \text{rank}(\boldsymbol{F}_k^\star)$ and $\text{rank}(\boldsymbol{\Psi}_k) = N - \text{rank}(\boldsymbol{G}_k^\star)$, then the following result is true

$$\text{rank}\,(\boldsymbol{\Omega}_k) \leq \text{rank}\,(\boldsymbol{\Psi}_i) + 1. \tag{45}$$

Now, let us examine the null space of $\boldsymbol{G}_k^\star$, $\boldsymbol{\psi}_{k,j} \in \boldsymbol{\Psi}_k$, by computing the inner product between $\boldsymbol{\psi}_{k,j}$ and $\boldsymbol{F}_k^\star$ in (43) as follows

$$\boldsymbol{\psi}_{k,j}^H \boldsymbol{F}_k^\star \boldsymbol{\psi}_{k,j} = -\boldsymbol{\psi}_{k,j}^H \left(\lambda_{2_k}^\star \tau^2 P_I \boldsymbol{A}_k\right) \boldsymbol{\psi}_{k,j} \leq 0, \tag{46}$$

where the inequality in (46) follows from[10] $\boldsymbol{A}_k \succeq 0$. However, since $\boldsymbol{F}_k^\star \succeq 0$, (46) can only hold with equality, i.e., $\boldsymbol{\psi}_{k,j}^H \left(\lambda_{2_k}^\star \tau^2 P_I \boldsymbol{A}_k\right) \boldsymbol{\psi}_{k,j} = 0$. This result implies that the null space of $\boldsymbol{G}_k^\star$ always forms the null space of $\boldsymbol{F}_k^\star$, i.e., $\boldsymbol{\Psi}_k$ is a sub-matrix of $\boldsymbol{\Omega}_k$, therefore, and according to (45), $\boldsymbol{\omega}_{k,j} \in \boldsymbol{\Omega}_k$ belongs to one of the following two spaces: 1) the column space of $\boldsymbol{\Psi}_k$, $\boldsymbol{\omega}_{k,j} \in \{\boldsymbol{\psi}_{k,j}\}$; 2) 1-dimensional vector space, $\boldsymbol{\omega}_{k,j} = \boldsymbol{a} \in \mathcal{C}^{N\times 1}$ where $\boldsymbol{a} \notin \{\boldsymbol{\psi}_{k,j}\}$.

Since the optimal value of $\boldsymbol{P}_k^\star$ needs to satisfy the complementary slackness condition, $\text{tr}(\boldsymbol{P}_k^\star \boldsymbol{F}_k^\star) = 0,\ \forall k$, the structure of $\boldsymbol{P}_k^\star$ is

$$\boldsymbol{P}_k^\star = \sum_{i=1}^{L\leq N} m_{k,j} \boldsymbol{q}_j \boldsymbol{q}_j^H, \quad \boldsymbol{q}_j \in \{\boldsymbol{\psi}_{k,j},\ \boldsymbol{a}\}, \tag{47}$$

where $\{m_{k,j}\}$ are non-negative scaling factors. The $\boldsymbol{P}_k^\star$'s component $m_{k,j}\boldsymbol{\psi}_{k,j}\boldsymbol{\psi}_{k,j}^H$ introduces zero information signal power at IU$_k$ since $\boldsymbol{\psi}_{k,j}^H \boldsymbol{A}_k \boldsymbol{\psi}_{k,j} = 0$, and therefore contributes by a negative ESR. Thus, $m_{k,j}\boldsymbol{\psi}_{k,j}\boldsymbol{\psi}_{k,j}^H$ is a non-optimal component of $\boldsymbol{P}_k^\star$. By this, we can conclude that $\boldsymbol{P}_k^\star$ is constructed by the single component $\boldsymbol{P}_k^\star = m_{k,1}\boldsymbol{a}\boldsymbol{a}^H$, $\boldsymbol{a} \notin \{\boldsymbol{\psi}_{k,j}\}$, therefore, $\text{rank}(\boldsymbol{P}_k^\star) = 1$ is always true. This concludes the proof.

REFERENCES

[1] G. Interdonato, E. Björnson, H. Q. Ngo, P. Frenger, and E. G. Larsson, "Ubiquitous cell-free massive MIMO communications," *arXiv preprint arXiv:1804.03421*, Oct. 2018.

[2] H. Q. Ngo, A. Ashikhmin, H. Yang, E. G. Larsson, and T. L. Marzetta, "Cell-free massive MIMO versus small cells," *IEEE Trans. Wireless Commun.*, vol. 16, no. 3, pp. 1834–1850, Mar. 2017.

[3] M. Jaber, M. A. Imran, R. Tafazolli, and A. Tukmanov, "A Distributed SON-based user-centric backhaul provisioning scheme," *IEEE Access*, vol. 4, pp. 2314–2330, 2016.

[4] X. Ge, H. Cheng, M. Guizani, and T. Han, "5G wireless backhaul networks: challenges and research advances," *IEEE Network*, vol. 28, no. 6, pp. 6–11, Nov. 2014.

[5] D. Kapetanovic, G. Zheng, and F. Rusek, "Physical layer security for massive MIMO: An overview on passive eavesdropping and active attacks," *IEEE Commun. Mag.*, vol. 53, no. 6, pp. 21–27, Jun. 2015.

[6] Y. Zeng and R. Zhang, "Active eavesdropping via spoofing relay attack," in *2016 IEEE International Conference on Acoustics, Speech and Signal Processing (ICASSP)*. IEEE, Mar. 2016, pp. 2159–2163.

[9]Please note that rank$(\boldsymbol{A}_k) = 1$, this is understandable from the structure of $\boldsymbol{A}_k$. Please refer to the first paragraph in IV-B.

[10]$\boldsymbol{A}_k \succeq 0$ follows since it is structured from a vector whose all entries are positive (see (25) and the paragraph that follows).

[7] A. Mukherjee, S. A. A. Fakoorian, J. Huang, and A. L. Swindlehurst, "Principles of physical layer security in multiuser wireless networks: A survey," *IEEE Commun. Surveys & Tutorials*, vol. 16, no. 3, pp. 1550–1573, Aug. 2014.

[8] J. Zhang, C. Yuen, C.-K. Wen, S. Jin, K.-K. Wong, and H. Zhu, "Large system secrecy rate analysis for SWIPT MIMO wiretap channels," *IEEE Trans. Inf. Forensics Security*, vol. 11, no. 1, pp. 74–85, Jan. 2016.

[9] Y. Zhu, L. Wang, K.-K. Wong, S. Jin, and Z. Zheng, "Wireless power transfer in massive MIMO-aided HetNets with user association," *IEEE Trans. Commun.*, vol. 64, no. 10, pp. 4181–4195, Oct. 2016.

[10] N. Nguyen, H. Q. Ngo, T. Q. Duong, H. D. Tuan, and K. Tourki, "Secure massive MIMO with the artificial noise-aided downlink training," *IEEE J. Sel. Areas Commun.*, vol. 36, no. 4, pp. 802–816, Apr. 2018.

[11] M. Alageli, A. Ikhlef, and J. Chambers, "SWIPT massive MIMO systems with active eavesdropping," *IEEE Journal on Selected Areas in Communications*, vol. 37, no. 1, pp. 233–247, Jan. 2019.

[12] L. D. Nguyen, T. Q. Duong, H. Q. Ngo, and K. Tourki, "Energy efficiency in cell-free massive MIMO with zero-forcing precoding design," *IEEE Commun. Lett.*, vol. 21, no. 8, pp. 1871–1874, Aug. 2017.

[13] T. H. Nguyen, T. K. Nguyen, H. D. Han, and V. D. Nguyen, "Optimal power control and load balancing for uplink cell-free multi-user massive MIMO," *IEEE Access*, vol. 6, pp. 14 462–14 473, Apr. 2018.

[14] H. Q. Ngo, L. Tran, T. Q. Duong, M. Matthaiou, and E. G. Larsson, "On the total energy efficiency of cell-free massive MIMO," *IEEE Trans. on Green Commun. and Netw.*, vol. 2, no. 1, pp. 25–39, Mar. 2018.

[15] T. M. Hoang, H. Q. Ngo, T. Q. Duong, H. D. Tuan, and A. Marshall, "Cell-free massive MIMO networks: optimal power control against active eavesdropping," *IEEE Trans. Commun.*, vol. 66, no. 10, pp. 4724–4737, Oct. 2018.

[16] G. Chen, Z. Tian, Y. Gong, Z. Chen, and J. A. Chambers, "Max-ratio relay selection in secure buffer-aided cooperative wireless networks," *IEEE Trans. Inf. Forensics Security*, vol. 9, no. 4, pp. 719–729, Apr. 2014.

[17] L. Liu, R. Zhang, and K. C. Chua, "Secrecy wireless information and power transfer with MISO beamforming," *IEEE Trans. Signal Process.*, vol. 62, no. 7, pp. 1850–1863, April 2014.

[18] C. Young, *Information security science: measuring the vulnerability to data compromises*. Syngress, 2016.

[19] X. Zhou, B. Maham, and A. Hjorungnes, "Pilot contamination for active eavesdropping," *IEEE Trans. Wireless Commun.*, vol. 11, no. 3, pp. 903–907, Mar. 2012.

[20] A. K. Jagannatham, "NOC: Estimation for wireless communications: MIMO/OFDM cellular and sensor networks," 2016, [Online] Available: http://nptel.ac.in/courses/117104118/ [Accessed: 2 Dec. 2017].

[21] S. M. Kay, *Fundamentals of statistical signal processing, volume I: Estimation theory*. Englewood Cliffs, PTR Prentice-Hall, 1993.

[22] J. K. Tugnait, "Pilot spoofing attack detection and countermeasure," *IEEE Trans. Commun.*, vol. 66, no. 5, pp. 2093–2106, May 2018.

[23] ——, "Detection and identification of spoofed pilots in TDD/SDMA systems," *IEEE Wireless Commun. Lett.*, vol. 6, no. 4, pp. 550–553, Aug. 2017.

[24] W. Zhang, H. Lin, and R. Zhang, "Detection of pilot contamination attack based on uncoordinated frequency shifts," *IEEE Trans. Commun.*, vol. 66, no. 6, pp. 2658–2670, Jan. 2018.

[25] J. Jose, A. Ashikhmin, T. L. Marzetta, and S. Vishwanath, "Pilot contamination and precoding in multi-cell TDD systems," *IEEE Trans. Wireless Commun.*, vol. 10, no. 8, pp. 2640–2651, Aug. 2011.

[26] G. Interdonato, H. Q. Ngo, E. G. Larsson, and P. Frenger, "How much do downlink pilots improve cell-free massive MIMO?" in *Global Commun. Conf. (GLOBECOM)*. IEEE, Dec. 2016, pp. 1–7.

[27] D. Tse and P. Viswanath, *Fundamentals of wireless communication*. Cambridge University Press, May 2005.

[28] Y. Wu, R. Schober, D. W. K. Ng, C. Xiao, and G. Caire, "Secure massive MIMO transmission with an active eavesdropper," *IEEE Trans. Inf. Theory*, vol. 62, no. 7, pp. 3880–3900, Jul. 2016.

[29] M. Alageli, A. Ikhlef, and J. Chambers, "Optimization for maximizing sum Secrecy rate in MU-MISO SWIPT systems," *IEEE Trans. Veh. Technol.*, vol. 67, no. 99, pp. 537–553, Sep. 2017.

[30] ——, "Optimal transmit power minimization in secure MU-MISO SWIPT systems," in *Proc. IEEE Int. Conf. Ubiquitous Wireless Broadband (ICUWB), Salamanca, Spain*, Sep. 2017, pp. 1–7.

[31] Z. Luo, W. Ma, A. M. So, Y. Ye, and S. Zhang, "Semidefinite relaxation of quadratic optimization problems," *IEEE Signal Processing Magazine*, vol. 27, no. 3, pp. 20–34, May 2010.

[32] M. Grant and S. Boyd, "CVX: Matlab software for disciplined convex programming, version 1.21, Apr. 2011," *Available: cvxr. com/cvx*.

[33] Y. Huang and D. P. Palomar, "Rank-Constrained separable semidefinite programming with applications to optimal beamforming," *IEEE Trans. Signal Process.*, vol. 58, no. 2, pp. 664–678, Feb. 2010.
[34] M. Alageli, A. Ikhlef, F. Alsifiany, M. A. M. Abdullah, G. Chen, and J. Chambers, "Optimal downlink transmission for cell free SWIPT massive MIMO systems with active eavesdropping," [Online]. Available: http://arxiv.org/abs/1904.11033.
[35] T. S. Rappaport *et al.*, *Wireless communications: principles and practice*. prentice hall PTR New Jersey, 1996, vol. 2.
[36] T. Le, K. Mayaram, and T. Fiez, "Efficient far-field radio frequency energy harvesting for passively powered sensor networks," *IEEE J. Solid-State Circuits*, vol. 43, no. 5, pp. 1287–1302, May 2008.
[37] J. Evans and D. N. C. Tse, "Large system performance of linear multiuser receivers in multipath fading channels," *IEEE Trans. Inf. Theory*, vol. 46, no. 6, pp. 2059–2078, Sep. 2000.
[38] G. Hamedani and G. Walter, "On the product of symmetric random variables," *Statistics & probability lett.*, vol. 3, no. 5, pp. 251–253, Sep. 1985.
[39] R. Chen and L. A. Shepp, "On the sum of symmetric random variables," *The American Statistician*, vol. 37, no. 3, pp. 237–237, Aug. 1983.
[40] D. Berend and T. Tassa, "Improved bounds on Bell numbers and on moments of sums of random variables," *Probability and Mathematical Statistics*, vol. 30, no. 2, pp. 185–205, Jan. 2010.
[41] J. Yuan, M. Matthaiou, S. Jin, and F. Gao, "Tightness of Jensen's bounds and applications to MIMO communications," *IEEE Trans. Commun.*, vol. 65, no. 2, pp. 579–593, Feb. 2017.
[42] G. Van Kempen and L. Van Vliet, "Mean and variance of ratio estimators used in fluorescence ratio imaging," *Cytometry Part A*, vol. 39, no. 4, pp. 300–305, Apr. 2000.
[43] J. E. Gentle, *Matrix algebra: theory, computations, and applications in statistics*. Springer Nature, 2017.

Aissa Ikhlef (M'09, SM'17) was born in Constantine, Algeria. He received the B.S. degree in Electrical Engineering from the University of Constantine, Constantine, Algeria, in 2001 and the M.Sc. and Ph.D. degrees in Electrical Engineering from the University of Rennes 1, Rennes, France, in 2004 and 2008, respectively. From 2004 to 2008, he was with Supélec, France, pursuing his Ph.D. degree. From 2007 to 2008, he was a Lecturer at the University of Rennes 1. From 2008 to 2010 he was a Postdoctoral Fellow with the Communication and Remote Sensing Laboratory, Catholic University of Louvain, Louvain La Neuve, Belgium. He was a visiting Postdoctoral Fellow at the University of British Columbia, Vancouver, BC, Canada, from August to November 2009. From 2010 to 2013 he was with the data communications group, University of British Columbia, Vancouver, Canada, as a Postdoctoral Fellow. From June 2013 to August 2014 he was with Toshiba Research Europe Limited, Bristol, UK, as a Senior Research Engineer. From September 2014 to August 2016 he was with the School of Electrical and Electronic Engineering, Newcastle University, Newcastle, UK, as a Lecturer (Assistant Professor). Since September 2016 he has been an Assistant Professor with the Department of Engineering, Durham University, Durham, UK. He served as an Editor for IEEE Communications Letters from 2014 to 2016. His current research interests include machine learning, energy harvesting communications, physical layer security, and massive MIMO.

Fahad Alsifiany received the B.Sc. degree in electrical and electronic engineering from King Abdulaziz University, Jeddah, Saudi Arabia, in 2000, and the M.Sc. degree in telecommunications and networking from the University of Pittsburgh, Pittsburgh, USA, in 2011. He is currently pursuing the Ph.D. degree with the Intelligent Sensing and Communications Group, Newcastle University, Newcastle upon Tyne, U.K. From 2001 to 2015, he was a Lecturer with the Faculty of the King Fahad Security College, Riyadh, Saudi Arabia. His current research interests include noncoherent systems, physical layer security, and massive multiple-input multiple-output (MIMO).

Mahmoud Alageli was born in Houn, Libya. He received the B.Sc. degree (Hons.) in Electrical and Electronic Engineering from the Engineering Academy Tajoura, Tripoli, Libya, in 1999, the M.Eng. degree in Communication and Computer from the National University of Malaysia, Malaysia, in 2006, and the Ph.D. degree in Communications and Signal Processing from Newcastle University, Newcastle upon Tyne, U.K., in 2019. From 2007 to 2011, he was an Assistant Lecturer with the Engineering Academy Tajoura. Since 2012 he has been a Lecturer with the Faculty of Engineering, Garaboulli, Elmergib University, Libya. His current research interests include energy harvesting communications, physical layer security, and massive MIMO. He was a recipient of the "The Bright Bestowal 2006" organized by the Center of Graduate Studies, National University of Malaysia.

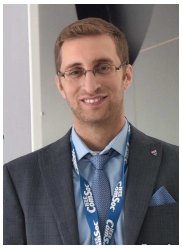

Mohammed A. M. Abdullah (M'10) received the PhD degree in 2017 from the School of Electrical and Electronic Engineering at Newcastle University, UK. He received the BSc and MSc degrees in Computer Engineering in 2008 and 2010, respectively from the University of Mosul, Iraq. During 2018, he worked as a post-doctorate researcher in the Department of Engineering at the University of Leicester, UK. He is currently a lecturer with the Department of Computer Engineering at Ninevah University. His research interests are in the fields of biometrics, machine learning, signal processing and wireless communication. Dr. Abdullah is a member of the IEEE, International Biometric Society (IBS) and the British Machine Vision Association (BMVA). He is also an associate fellow of the UK Higher Education Academy (AFHEA).

Gaojie Chen (S'09-M'12-SM'18) received the B.Eng. and B.Ec. degrees in electrical information engineering and international economics and trade from Northwest University, China, in 2006, and the M.Sc. (Hons.) and Ph.D. degrees in electrical and electronic engineering from Loughborough University, Loughborough, U.K., in 2008 and 2012, respectively. From 2008 to 2009, he was a Software Engineering with DTmobile, Beijing, China, and from 2012 to 2013, he was a Research Associate with the School of Electronic, Electrical and Systems Engineering, Loughborough University. He was a Research Fellow with 5GIC, Faculty of Engineering and Physical Sciences, University of Surrey, U.K., from 2014 to 2015. Then he was a Research Associate with the Department of Engineering Science, University of Oxford, U.K., from 2015 to 2018. He is currently a Lecturer with the Department of Engineering, University of Leicester, U.K.

His current research interests include information theory, wireless communications, cooperative communications, cognitive radio, secrecy communication, and random geometric networks. He received the Exemplary Reviewer Certificate of the IEEE Wireless Communication Letters in 2018. He has served as an Editor for IET ELECTRONICS LETTERS (2018-present).

Jonathon Chambers (S'83–M'90–SM'98–F'11) received the Ph.D. and D.Sc. degrees in signal processing from the Imperial College of Science, Technology and Medicine (Imperial College London), London, U.K., in 1990 and 2014, respectively. From 1991 to 1994, he was a Research Scientist with the Schlumberger Cambridge Research Center, Cambridge, U.K. In 1994, he returned to Imperial College London as a Lecturer in signal processing and was promoted to Reader (Associate Professor) in 1998. From 2001 to 2004, he was the Director of the Center for Digital Signal Processing and a Professor of signal processing with the Division of Engineering, King's College London and is now a Visiting Professor. From 2004 to 2007, he was a Cardiff Professorial Research Fellow with the School of Engineering, Cardiff University, Cardiff, U.K. Between 2007–2014, he led the Advanced Signal Processing Group, within the School of Electronic, Electrical and Systems Engineering, Loughborough University, and is now a Visiting Professor. From 2015 to 2017, he joined the School of Electrical and Electronic Engineering, from the 1st Aug 2017 the School of Engineering, Newcastle University, where he was a Professor of signal and information processing and led the Intelligent Sensing and Communications group, and is now a Visiting Professor. On 1st Dec 2017 he became the Head of the Engineering Department at the University of Leicester. He is also an International Honorary Dean and Guest Professor within the Department of Automation at Harbin Engineering University, China. He has advised more than 80 researchers through to Ph.D. graduation and published more than 500 conference proceedings and journal articles, many of which are in IEEE journals. His research interests include adaptive signal processing and machine learning and their application in communications, defence and navigation systems.

Dr. Chambers is a Fellow of the Royal Academy of Engineering, U.K., the Institution of Engineering and Technology, and the Institute of Mathematics and its Applications. He was a Technical Program Co-chair for the 36th IEEE International Conference on Acoustics, Speech, and Signal Processing (ICASSP), Prague, Czech Republic and is serving on the organising committees of ICASSP 2019 Brighton, UK, and ICASSP 2022, Singapore. He has served on the IEEE Signal Processing Theory and Methods Technical Committee for six years, the IEEE Signal Processing Society Awards Board for three years, and the Jack Kilby Medal Commitee for three years. He has also served as an Associate Editor for the IEEE TRANSACTIONS ON SIGNAL PROCESSING for three terms over the periods 1997–1999, 2004–2007, and as a Senior Area Editor 2011–2015.